

A Kinetic Model for Distinguishing between Direct and Indirect Interfacial Hole Transfer in the Heterogeneous Photooxidation of Dissolved Organics on TiO₂ Nanoparticle Suspensions

Teresa Lana Villarreal,^{†,‡} Roberto Gómez,[‡] M. González,[#] and P. Salvador^{*,†,#}

Instituto de Catálisis y Petroleoquímica, CSIC, Madrid, Spain, Departament de Química Física and Institut Universitari d'Electroquímica, Universitat d'Alacant, Ap. 99, E-03080 Alacant, Spain, and Departament de Ciències Matemàtiques i Informàtica, Universitat Illes Balears, E-07122 Palma, Spain

Received: August 2, 2004; In Final Form: September 27, 2004

A kinetic model for assessing the photocatalytic degradation of water-dissolved pollutant species at suspensions of TiO₂ nanoparticles is presented. The model is based on the sequence of reactions occurring at the semiconductor/electrolyte interface under illumination, and emphasizes the degree of electronic interaction of dissolved pollutant species with the semiconductor surface. In the case of weak interaction (nonspecific adsorption), the model establishes that interfacial hole transfer takes place via an isoenergetic, indirect mechanism involving photogenerated surface-bound OH• radicals. In contrast, for strong interaction (specific adsorption), interfacial hole transfer takes place via a mixture of the indirect mechanism and an inelastic, direct one involving photogenerated valence band free holes, which predominates for low enough photon fluxes. Under high illumination intensity (standard experimental conditions), a linear dependence of the photodegradation quantum yield (QY) on the inverse of the square root of the photon flux, ϕ (i.e., $\text{QY} \propto \phi^{-1/2}$), is predicted for indirect hole transfer (nonspecific adsorption), while a ϕ independent QY is predicted for direct hole transfer. The quantum yield dependence on the pollutant concentration for strong interaction is determined by the type of adsorption. So, for a Langmuir adsorption type, a linear dependence of the inverse of the QY on the inverse of the pollutant concentration ($\text{QY}^{-1} \propto [\text{RH}_2]_{\text{aq}}^{-1}$) is predicted. On the other hand, in the absence of specific adsorption a linear dependence of the inverse of the QY on the inverse of the square root of the pollutant concentration ($\text{QY}^{-1} \propto [\text{RH}_2]_{\text{aq}}^{-1/2}$) is obtained for high enough illumination intensity. The predicted behavior has been contrasted with literature experimental data.

1. Introduction

Semiconductor photocatalysis has been proven to have important applications as an environmental control technology. As established in a recent report, the number of publications (including patents) in this field from 1970 to the middle of 2001 is more than 6200.¹ Attention has been mainly devoted to the photodegradation of water-dissolved organic compounds (pollutants) using suspensions of TiO₂ nanoparticles. Most of these photodegradation reactions take advantage of the extremely high oxidizing power of valence band photogenerated holes to degrade the pollutants, dissolved oxygen acting as an efficient scavenger for conduction band photogenerated electrons. This means that in the absence of O₂ (or another electron scavenger) the photooxidation rate of dissolved pollutant species decreases dramatically.² Concerning the photooxidation mechanisms, a question still open is whether interfacial hole transfer takes place directly via photogenerated valence-band free holes, or indirectly, via holes trapped at surface-bound OH• radicals. The nature of the interfacial hole transfer mechanism, either direct or indirect, is in many cases one of the objects of controversy,

mainly due to the lack of experimental techniques able to give an unambiguous response.^{3–23}

Specific adsorption of dissolved pollutant species, $(\text{RH}_2)_{\text{aq}}$, on the TiO₂ surface seems to play an important role in determining photoreactivity.^{19,24} Numerous researchers have reported that the rate of photodegradation of chemical compounds in suspensions of semiconductor nanoparticles, including TiO₂, follows the classical Langmuir–Hinshelwood (LH) mechanism.^{5,25–40} The LH model establishes that under Langmuir type adsorption conditions the photodegradation rate, v_{ox} , depends on the concentration of dissolved pollutant species, $[(\text{RH}_2)_{\text{aq}}]$, according to the relationship: $v_{\text{ox}} = k_{\text{ox}}K[(\text{RH}_2)_{\text{aq}}]/[1 + K(\text{RH}_2)_{\text{aq}}]$, where k_{ox} is the photooxidation rate constant and K the equilibrium adsorption constant. This relationship can also be written as $1/v_{\text{ox}} = 1/k_{\text{ox}}K[(\text{RH}_2)_{\text{aq}}] + 1/k_{\text{ox}}$, which establishes a linear dependence between the inverse of the photodegradation rate and the inverse of the dissolved pollutant concentration. However, the LH model is not able to define a relationship between v_{ox} and the illumination intensity, ϕ , unless the dependence of k_{ox} on ϕ is known. In this respect, Hoffmann et al.⁵ have claimed that according to the LH kinetics the photodegradation quantum yield (QY) at high enough illumination intensities (standard experimental conditions) depends linearly on the inverse of the square root of the absorbed photon flux, ϕ (i.e., $\text{QY} \propto \phi^{-1/2}$), irrespective of the prevailing interfacial hole transfer mechanism, either direct or indirect. This dependence has been attributed to the enhanced band gap

* Corresponding author: Departament de Ciències Matemàtiques i Informàtica, Universitat de les Illes Balears. Crt. de Valldemossa Km. 7.5, E-07122 Palma de Mallorca, Spain. Tel.: +34 971 172962. Fax.: +34 971 173003. E-mail: dmipss9@uib.es.

[†] Instituto de Catálisis y Petroleoquímica.

[‡] Universitat d'Alacant.

[#] Universitat Illes Balears.

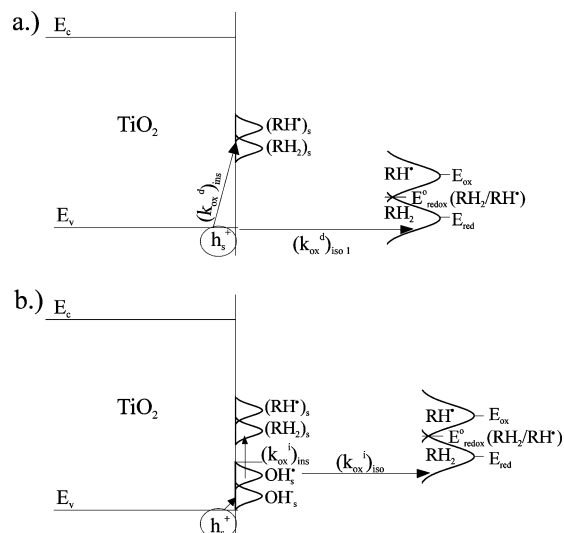


Figure 1. Diagrams showing semiconductor and electrolyte energy levels, for (a) direct (d) and (b) indirect (i), interfacial hole transfer to water molecules and to dissolved RH_2 pollutant species. The hole transfer mechanism can be either isoenergetic (iso), represented by horizontal arrows, or inelastic (ins). Marcus-Gerischer fluctuating energy model for isoenergetic charge transfer only applies for weak electronic interaction of electrolyte species with the semiconductor surface (absence of specific adsorption). For the case of specific adsorption (strong interaction) interfacial hole transfer is inelastic and the activation energy term of Marcus-Gerischer model disappears.

recombination in the case of direct hole transfer,^{41–43} and to the chemical reaction between photogenerated surface-bound radicals in the case of indirect hole transfer.⁴⁴ Turchi and Ollis have also shown that the LH model presents a high degree of ambiguity, as different reactions schemes can be compatible with a unique rate equation.⁴⁵ Recent photocatalytic degradation studies have shown that in many cases the quantum yield is light intensity independent, even for high ϕ values, which contradicts LH model predictions. Some examples of this behavior concern the photooxidative degradation of formic acid,⁴⁶ chlorophenol,⁴⁷ and dimethyl-pyrroline *N*-oxide.⁴⁸

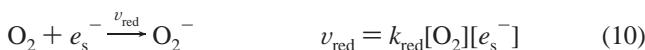
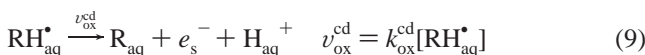
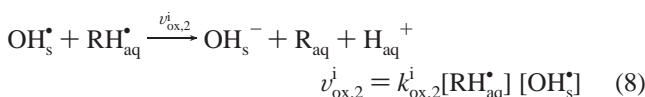
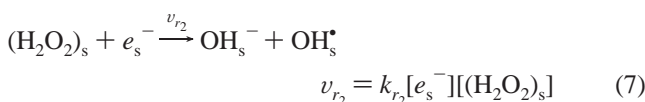
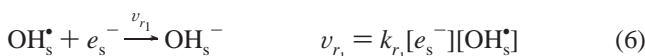
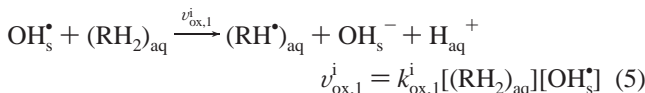
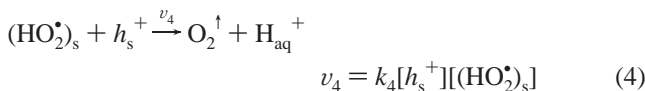
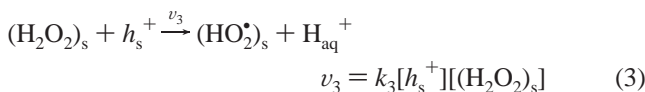
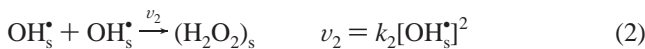
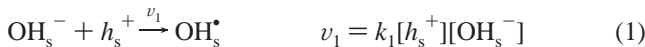
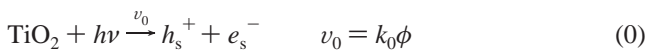
Recently, we have developed a kinetic model that allows us to distinguish between direct and indirect interfacial hole transfer from photoelectrochemical measurements concerning the photooxidation of water dissolved pollutants at polycrystalline anatase thin films.⁴⁹ This model is based on the general premise that the photooxidative degradation of dissolved pollutant species takes place in competition with the photooxidation of the solvent (water molecules). The model emphasizes the important role that the interaction pollutant/semiconductor surface plays in determining whether interfacial hole transfer takes place either directly or indirectly. The main features of the model are schematized in Figure 1. Figure 1a concerns direct (d) hole transfer. Two limiting cases can be considered: either weak or strong interaction of RH_2 species with the semiconductor surface. In the first case (absence of specific adsorption), isoenergetic (iso) interfacial hole transfer is highly favored. According to the Marcus-Gerischer fluctuating energy model,⁵⁰ the rate constant for isoenergetic hole transfer from valence band energy levels near E_v to dissolved species interacting weakly with the semiconductor surface (outside the Helmholtz layer), $(k_{\text{ox}}^{\text{d}})_{\text{iso}}$, includes an activation energy term that takes into account the reorganization of the $\text{RH}_2\text{-H}_2\text{O}$ structure. $(k_{\text{ox}}^{\text{d}})_{\text{iso}}$ decreases exponentially with the square of the energy difference between filled electronic states of RH_2 species, E_{red} , and empty valence band, electronic states located just below E_v ($(k_{\text{ox}}^{\text{d}})_{\text{iso}} \propto$

$\exp(-(E_{\text{red}} - E_v)^2/4\lambda kT)$, λ being the reorganization energy for the transformation $\text{RH}_2 + \text{h}^+ \rightarrow \text{RH}^\bullet + \text{H}^+$). Because of the very positive value of E_v for TiO_2 , except for the case of very reductant dissolved species, $(E_{\text{red}} - E_v)$ reaches typical values of more than 1 eV (e.g., about 2 eV for the $\text{H}_3\text{COH}/\text{H}_2\text{COH}^\bullet$ redox couple),⁵¹ resulting in an extremely small $(k_{\text{ox}}^{\text{d}})_{\text{iso}}$ and a negligible probability of isoenergetic, direct hole transfer. In contrast, for the case of strong electronic interaction (specific adsorption), direct hole transfer to band gap energy levels, $E_{(\text{RH}_2)_s}$, associated with specifically adsorbed $(\text{RH}_2)_s$ species takes place inelastically (ins), i.e., with hole energy loss. In this case, the activation energy term (exponential term of $(k_{\text{ox}}^{\text{d}})_{\text{iso}}$) disappears,⁴⁹ and the rate constant for inelastic hole transfer, $(k_{\text{ox}}^{\text{d}})_{\text{ins}}$, increases drastically with respect to $(k_{\text{ox}}^{\text{d}})_{\text{iso}}$. The conclusion is that, in general, direct hole transfer will be restricted to the case of specific adsorption. Exceptionally, for nonspecifically adsorbed species, like bifunctional aromatics,⁵² where $E_{\text{red}} \approx E_v$, $(k_{\text{ox}}^{\text{d}})_{\text{iso}}$ can reach values comparable to $(k_{\text{ox}}^{\text{d}})_{\text{ins}}$ and an efficient direct hole transfer mechanism will be possible. Figure 1b refers to indirect (i) hole transfer via holes trapped at surface-bound OH_s^\bullet radicals. If specific adsorption is assumed the hole transfer mechanism would be also inelastic; however, because of the expected low mobility of surface-bound OH_s^\bullet species,⁵³ the inelastic, indirect hole transfer rate constant, $(k_{\text{ox}}^{\text{i}})_{\text{ins}}$, should be extremely small, unless both reacting species, OH_s^\bullet and $(\text{RH}_2)_s$, were adsorbed close together on adjacent surface sites. The conclusion should be that an efficient indirect hole transfer mechanism would involve nonspecific adsorption. But in this case hole transfer should be isoenergetic, i.e., $(k_{\text{ox}}^{\text{i}})_{\text{iso}} \propto \exp(-(E_{\text{red}} - E_{\text{OH}_s^\bullet})^2/4\lambda kT)$, where $E_{\text{OH}_s^\bullet}$ represents band gap empty energy levels associated with surface-bound OH_s^\bullet radicals. Summing up, for the case of specific adsorption, direct hole transfer should, in general, predominate on indirect hole transfer, while in the absence of specific adsorption the dominant hole transfer mechanism should be indirect. Moreover, because of the existence of the activation energy term, unless $E_{\text{red}}(\text{RH}_2) \approx E_{\text{OH}_s^\bullet}$, it will be $(k_{\text{ox}}^{\text{i}})_{\text{iso}} \ll (k_{\text{ox}}^{\text{i}})_{\text{ins}}$, which means that, in general, the direct photooxidation mechanism should be more efficient than the indirect one.

These concepts constitute the base of a kinetic model able to discriminate between direct and indirect hole transfer from photoelectrochemical oxidation experiments with polycrystalline anatase thin film electrodes.⁴⁹ According to this model, it has been unequivocally shown that methanol, which is not specifically adsorbed on the TiO_2 surface, is photooxidized indirectly, while direct hole transfer dominates in the photooxidation of formic acid, which is adsorbed specifically. Here, an implemented version of this model is applied to the photocatalytic oxidation of water dissolved pollutants at suspensions of TiO_2 nanoparticles.

2. The Model in the Absence of Specific Adsorption. For the sake of clarity, we will not treat a total photomineralization case, but a partial photooxidation process involving the exchange of a couple of electrons. The oxidant species is considered to be dissolved oxygen.

The reaction scheme for the indirect photocatalytic oxidation of $(\text{RH}_2)_{\text{aq}}$ nonspecifically adsorbed species, via photogenerated surface-bound OH_s^\bullet radicals (eqs 0–10), is similar to that used previously for semiconductor electrodes under external potential bias,⁴⁹ except for the recombination reactions 6 and 7, which here should be taken into account because of the nonnegligible concentration of conduction band free electrons, $[e_s^-]$.



In general, the reaction rates defined by eqs 0–10 should be considered as initial reaction rates under quasi-steady-state conditions. This is a simplified reaction scheme not including other secondary mechanisms for the photooxidation of dissolved pollutant species, such as those taking place in the homogeneous phase via OH^\bullet and H_2O_2 species generated at intermediate steps of the electroreduction of dissolved oxygen. Because of the low initial concentration of these species, the rates of the corresponding photooxidation reactions are considered to be negligible vs $\nu_{\text{ox},1}^i$.

Eq 0 represents the photogeneration rate of electron-hole pairs within the nanoparticles, which depends linearly on the incident photon flux, ϕ ($\text{cm}^{-2} \text{s}^{-1}$). It has been shown that $\nu_0 = gR/3$, where R is the nanoparticles radius and g ($\text{cm}^{-3} \text{s}^{-1}$) is the light absorption rate; for $R \approx 10^{-6} \text{ cm}$ it is $k_0 \approx 10^{-3}$.⁵⁴ According to eq 1, photogenerated valence band free holes are trapped inelastically as surface-bound OH_s^\bullet radicals at a rate ν_1 ; this constitutes the first step of water photooxidation. Further, the combination of two OH_s^\bullet radicals adsorbed at neighboring surface sites leads to a surface-bound hydrogen peroxide molecule (eq 2).⁵⁵ In principle, photogenerated surface-bound $(\text{H}_2\text{O}_2)_s$ species can be either oxidized with valence band free holes (eq 3) or reduced with conduction band free electrons (eq 8). Finally, oxygen can be evolved according to eq 4. Equations 1, 3, and 4 involve a direct hole transfer mechanism, according to which valence band free holes are trapped inelastically by surface-bound OH_s^- , $(\text{H}_2\text{O}_2)_s$, and $(\text{HO}_2^\bullet)_s$ species, respectively. By contrast, eq 5 represents the photooxidation of dissolved RH_2 species via an isoenergetic, indirect hole transfer mechanism with the participation of surface trapped holes (OH_s^\bullet). The resulting $\text{RH}_{\text{aq}}^\bullet$ radicals are further photooxi-

dized either indirectly (eq 8) or by direct injection of an electron into the conduction band, via a “current doubling” (cd) mechanism represented by eq 9. In both cases, the electron transfer is isoenergetic, the ratio $(\nu_{\text{ox},2}^i/\nu_{\text{ox}}^{\text{cd}})$ depending on the degree of overlapping between filled energy levels associated with $\text{RH}_{\text{aq}}^\bullet$ dissolved species and either empty energy levels associated with OH_s^\bullet surfaces states (eq 8) or conduction band states (eq 9). Because of energetic restrictions, reactions 8 and 9 cannot take place simultaneously. In fact, for reaction 9 to take place a good overlapping of filled energy levels associated with $\text{RH}_{\text{aq}}^\bullet$ radicals and conduction band empty levels is necessary, which results in a very low probability for the isoenergetic transfer of charge involved in reaction 8. Recombination mechanisms are represented by eqs 6 and 7, which concern direct, interfacial electron transfer via inelastic trapping of free conduction band electrons by OH_s^\bullet and $(\text{H}_2\text{O}_2)_s$ surface-bound species (band gap surface states), respectively. The recombination rate via dissolved $\text{RH}_{\text{aq}}^\bullet$ species is considered to be negligible with respect to ν_{r1} , as the first reaction is indirect while the second one is direct. It should be realized that only in the case that $\nu_3 \geq \nu_{r2}$ (i.e., $k_3[h_s^+] \geq k_{r2}[e_s^-]$), photooxidation of water (oxygen evolution according to eq 4) will compete efficiently with RH_2 photooxidation. Finally, eq 10 takes into account the first step of the electroreduction of dissolved O_2 , which is considered to be rate-determining.^{46,56,58–61}

It is well-known that under illumination suspended nanoparticles can accumulate a certain excess of electrons.² However, this accumulation is limited, so that under quasi-steady-state conditions it should be assumed that $\nu_{\text{red}} \approx \nu_{\text{ox},1}^i$, which means that the rate of photooxidation of dissolved RH_2 species is limited by the rate of electroreduction of dissolved O_2 .

Let us define the surface concentration of OH_s^- species under equilibrium conditions in the dark as $[\text{OH}_s^-]_{\text{in}} \approx 10^{14}–10^{15} \text{ cm}^{-2}$, so that at the steady state under illumination it will be $[\text{OH}_s^-] + [\text{OH}_s^\bullet] + [(\text{H}_2\text{O}_2)_s] + [(\text{HO}_2^\bullet)_s] \approx [\text{OH}_s^-]_{\text{in}}$. Under standard experimental conditions, i.e., low enough illumination intensity ($\phi \leq 10^{16} \text{ cm}^{-2} \text{s}^{-1}$), it is reasonable to assume that $[\text{OH}_s^-] \gg [\text{OH}_s^\bullet] > [(\text{H}_2\text{O}_2)_s] > [(\text{HO}_2^\bullet)_s]$,⁵⁷ and, therefore, that $[\text{OH}_s^-] \approx [\text{OH}_s^-]_{\text{in}}$ (see eq 18 below).

On the other hand, under quasi-steady-state conditions we have that $d[h_s^+]/dt = \nu_0 - \nu_1 - \nu_3 - \nu_4 = 0$, and taking into account that for low enough illumination intensity (standard experimental conditions) $[\text{OH}_s^\bullet] \gg [(\text{H}_2\text{O}_2)_s]$, $[(\text{HO}_2^\bullet)_s]$, it will be $\nu_1 \gg \nu_3, \nu_4$, and therefore $\nu_0 \approx \nu_1$. Thus, the quasi-steady-state concentration of photogenerated valence band free holes becomes:

$$[h_s^+] \approx \frac{\nu_0}{k_1[\text{OH}_s^-]} \approx \frac{\nu_0}{k_1[\text{OH}_s^-]_{\text{in}}} \quad (11)$$

In the following, we will develop the model both in the absence and in the presence of the current doubling phenomenon.

2A. Presence of Current Doubling: $\nu_{\text{ox},2}^i = 0$. In this case, RH_s^\bullet is able to inject an electron into the conduction band of the semiconductor nanoparticle. Under quasi-steady-state conditions, we have that $d[h_s^+]/dt = \nu_0 - \nu_1 = 0$, $d[e_s^-]/dt = \nu_0 + \nu_{\text{ox}}^{\text{cd}} - \nu_{r1} - \nu_{\text{red}} = 0$, and $d[\text{RH}_s^\bullet]/dt = \nu_{\text{ox},1}^i - \nu_{\text{ox}}^{\text{cd}} = 0$; ν_{r2} has been neglected because $[(\text{H}_2\text{O}_2)_s]$ is considered to be significantly lower than $[\text{OH}_s^\bullet]$ under low enough standard experimental conditions.⁷ Therefore, the following expressions are deduced:

$$\nu_0 = k_1[\text{OH}_s^-][h_s^+] \quad (12)$$

$$v_{\text{ox},1}^i = v_{\text{ox}}^{\text{cd}} \quad (13)$$

$$[e_s^-] = \frac{v_0 + k_{\text{ox},1}^i [\text{RH}_2][\text{OH}_s^*]}{k_{r_1} [\text{OH}_s^*] + k_{\text{red}} [\text{O}_2]} \quad (14)$$

From 11 and 14, we have that $[e_s^-]/[h_s^+] \approx k_1 [\text{OH}_s^-]_{\text{in}} / (v_0 + v_{\text{ox},1}^i) / (k_{r_1} [\text{OH}_s^*] + k_{\text{red}} [\text{O}_2]) v_0 \gg 1$, even if $k_{\text{red}} [\text{O}_2] \gg k_{r_1} [\text{OH}_s^*]$, as $k_{\text{red}} [\text{O}_2] \ll k_1 [\text{OH}_s^-]_{\text{in}}$; thus $v_3 \ll v_{r_2}$ and, consequently, $v_2 \approx v_{r_2}$. This means that under standard experimental conditions $v_{\text{ox},1}^i \gg v_4$, i.e., that the rate of oxygen evolution (eq 4) can be considered to be negligible with respect to the rate of photooxidation of RH_2 dissolved species via surface-bound OH_s^* radicals (eq 5).

The quantum yield can be defined as

$$\text{QY} = \frac{\text{molecules of R produced}}{\text{absorbed photons}} = \frac{\text{molecules of } \text{RH}_2 \text{ oxidized}}{\text{photogenerated holes}} = \frac{v_{\text{ox}}^{\text{cd}}}{v_0} = \frac{v_{\text{ox},1}^i}{v_0} = \frac{k_{\text{ox},1}^i [(\text{RH}_2)_{\text{aq}}] [\text{OH}_s^*]}{k_0 \phi} \quad (15)$$

But under quasi-steady-state conditions

$$\frac{d[\text{OH}_s^*]}{dt} = v_1 - v_{\text{ox},1}^i - v_{r_1} = 0 \quad (16)$$

so that combining eqs 12, 14, and 16 we obtain

$$[\text{OH}_s^*] = \left\{ \left[\frac{k_{\text{ox},1}^i k_{\text{red}} [\text{O}_2] [(\text{RH}_2)_{\text{aq}}]^2}{8 k_{\text{ox},1}^i k_{r_1} k_{\text{red}} [\text{O}_2] [(\text{RH}_2)_{\text{aq}}] k_0 \phi} - k_{\text{ox},1}^i k_{\text{red}} [\text{O}_2] [(\text{RH}_2)_{\text{aq}}] \right\} / \left\{ 4 k_{\text{ox},1}^i k_{r_1} [(\text{RH}_2)_{\text{aq}}] \right\} \quad (17)$$

Finally, by substituting eq 17 into eq 15 the following expression for the quantum yield is obtained

$$\text{QY} = \left[\left(\frac{k_{\text{ox},1}^i k_{\text{red}} [\text{O}_2] [(\text{RH}_2)_{\text{aq}}]^2}{4 k_{r_1} k_0 \phi} \right) + \frac{k_{\text{ox},1}^i k_{\text{red}} [\text{O}_2] [(\text{RH}_2)_{\text{aq}}]}{2 k_{r_1} k_0 \phi} \right]^{1/2} - \frac{k_{\text{ox},1}^i k_{\text{red}} [\text{O}_2] [(\text{RH}_2)_{\text{aq}}]}{4 k_{r_1} k_0 \phi} \quad (18)$$

According to eq 18, it can be seen that $\text{QY} \rightarrow 1$ for $\phi \rightarrow 0$. Besides, for high enough illumination intensity ($\phi \gg k_{\text{ox},1}^i k_{\text{red}} [\text{O}_2] [(\text{RH}_2)_{\text{aq}}] / 8 k_{r_1} k_0$), the quantum yield becomes:

$$\text{QY} = \left[\frac{k_{\text{ox},1}^i k_{\text{red}} [\text{O}_2] [(\text{RH}_2)_{\text{aq}}]}{2 k_0 k_{r_1}} \right]^{1/2} \phi^{-1/2} \quad (19)$$

Equation 19 predicts a linear dependence of the quantum yield on the inverse of the square root of the illumination intensity, as frequently found in the literature experimental data.^{58,59,62–64} Moreover, from eqs 18 and 19 it can be stated that, in general, $\text{QY} \propto \phi^{-m}$, with $1/2 \geq m \geq 0$, so that a plot of $\log \text{QY}$ vs $\log \phi$ should show a slope ranging from zero for $\phi \rightarrow 0$ to $-1/2$ for high enough illumination intensity, as can be seen in Figure 2. Figure 2b shows the plot of $\log \text{QY}$ vs $\log \phi$ and Figure 2c the quantum yield vs $\phi^{-1/2}$. Furthermore, it can be seen that the higher $[(\text{RH}_2)_{\text{aq}}]$ the higher the illumination intensities needed

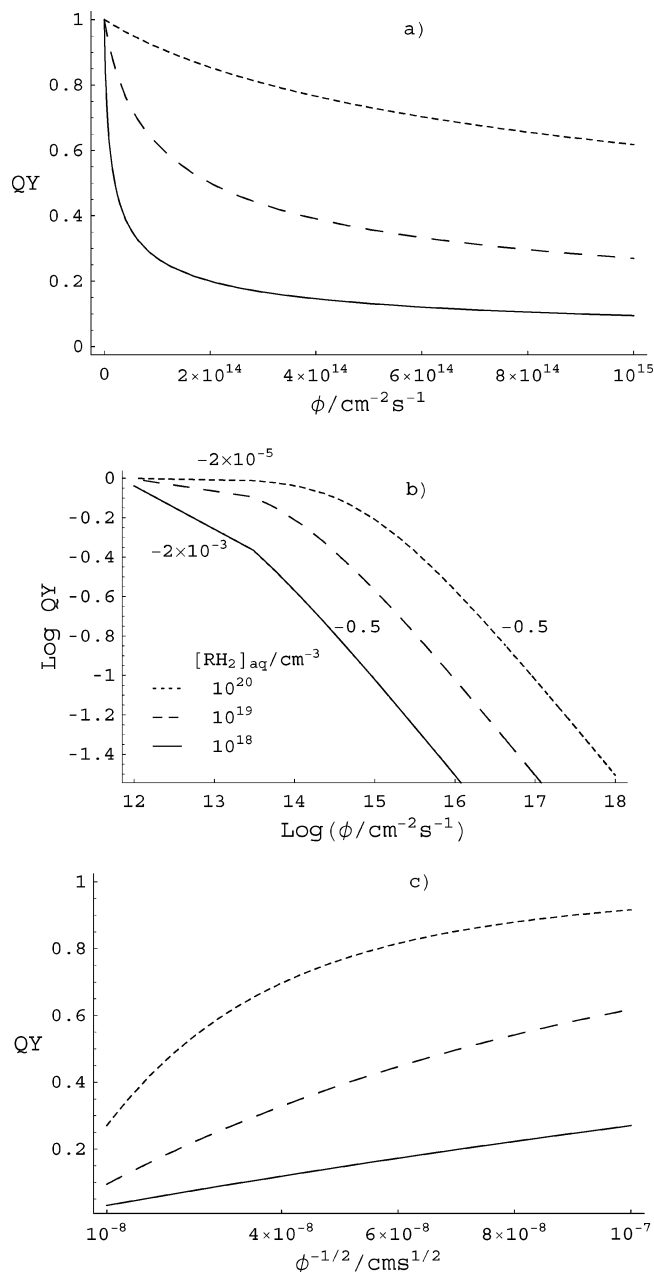


Figure 2. Influence of the pollutant concentration ($[(\text{RH}_2)_{\text{aq}}]$) on the dependence of the quantum yield (QY) on illumination intensity (ϕ) (linear plot (a) and logarithmic plot (b)) and $\phi^{-1/2}$ (c), according to eq 18, for $k_{\text{red}} [\text{O}_2] = 10^{-3} \text{ cm s}^{-1}$ (ref 2), $k_0 = 10^{-3}$ (ref 2), $k_{r_1} = 10^{-8} \text{ cm}^3 \text{ s}^{-1}$ (ref 56), and $k_{\text{ox},1}^i = 10^{-13} \text{ cm}^3 \text{ s}^{-1}$ (ref 50). The slopes ($\partial(\log \text{QY})/\partial(\log \phi)$) are indicated in (b).

to obtain a QY proportional to $\phi^{-1/2}$. The influence of the indirect hole transfer rate constant, $k_{\text{ox},1}^i$, on the illumination intensity dependence of the quantum yield is shown in Figure 3, where it can be seen that the lower $k_{\text{ox},1}^i$ the lower the photon flux needed for eq 19 (i.e., $\text{QY} \propto \phi^{-1/2}$) to hold.

The dependence of the quantum yield on the pollutant concentration for variable illumination intensity, according to eq 18, is shown in Figure 4a. As expected, for a LH mechanism $d\text{QY}/d[(\text{RH}_2)_{\text{aq}}]$ decreases as $[(\text{RH}_2)_{\text{aq}}]$ increases. However, as can be seen in Figure 4b, the Langmuir prediction that a plot of $1/\text{QY}$ vs $1/[(\text{RH}_2)_{\text{aq}}]$ should be linear is not fulfilled.

2B. Absence of Current Doubling: $v_{\text{ox}}^{\text{cd}} = 0$. In this case $d[e_s^-]/dt = v_0 - v_{r_1} - v_{r_2} - v_{\text{red}} = 0$, and considering that under low enough illumination intensity (standard experimental

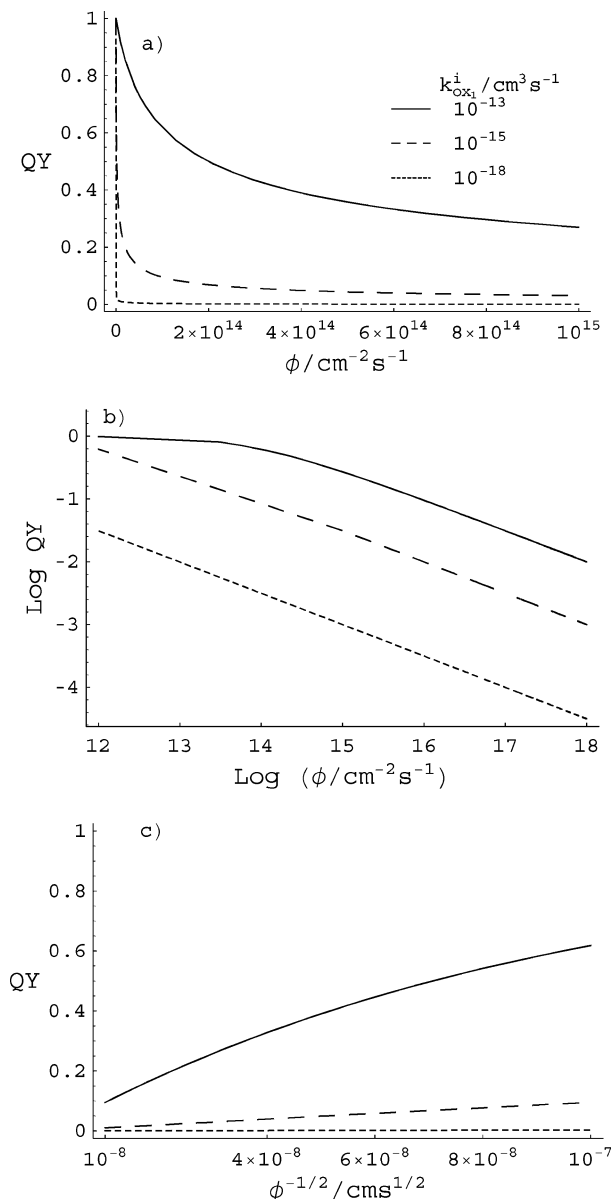


Figure 3. Influence of the indirect hole transfer rate constant, $k_{ox,1}^i$, on the dependence of the quantum yield (QY) on the illumination intensity (ϕ) (linear plot (a) and logarithmic plot (b)) and $\phi^{-1/2}$ (c), according to eq 18 ($k_{red}[\text{O}_2] = 10^{-3} \text{ cm s}^{-1}$, $k_o = 10^{-3}$, $k_{r1} = 10^{-8} \text{ cm}^3 \text{ s}^{-1}$ and $[(\text{RH}_2)_{aq}] = 10^{19} \text{ cm}^{-3}$).

conditions) $[\text{OH}_s^*] \gg [(\text{H}_2\text{O}_2)_s]$ ⁵⁷ and, therefore, $v_{r1} \gg v_{r2}$, it should be:

$$v_0 \approx v_{r1} + v_{red} \quad (20)$$

so that

$$[e_s^-] \approx \frac{v_0}{k_{r1}[\text{OH}_s^*] + k_{red}[\text{O}_2]} \quad (21)$$

From 11 and 21 we have that $[e_s^-]/[h_s^+] = k_1[\text{OH}_s^-]_{in}/(k_{r1}[\text{OH}_s^*] + k_{red}[\text{O}_2])$, and considering again that under low enough illumination intensity (standard experimental conditions) $[\text{OH}_s^*] \ll [\text{OH}_s^-]_{in}$,⁵⁷ we draw the conclusion that, in general, $[e_s^-] \gg [h_s^+]$ and $k_{red}[\text{O}_2] \ll k_1[\text{OH}_s^-]_{in}$. As in the current doubling case, the oxygen evolution rate (eq 4) can be considered to be negligible with respect to the rate of photo-

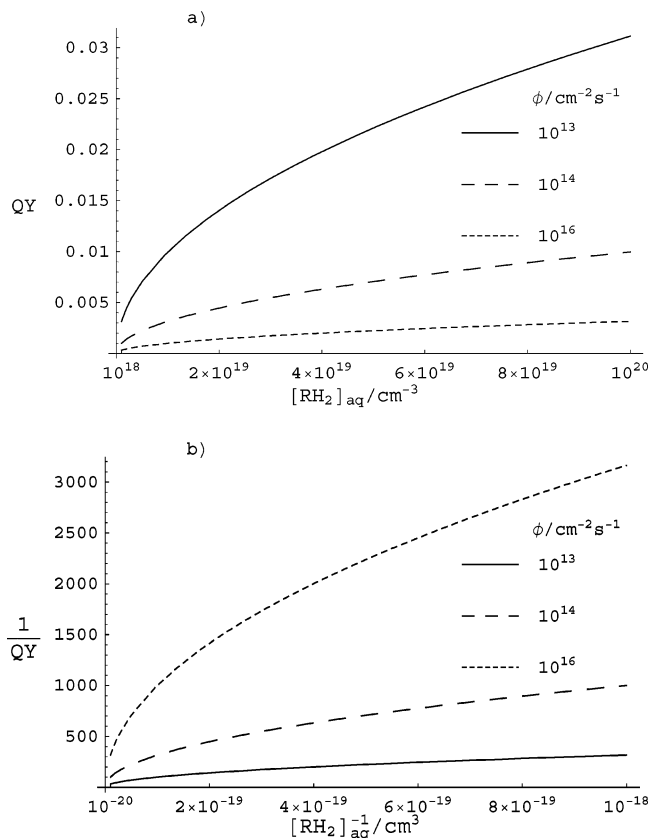


Figure 4. Plots of (a) quantum yield (QY) vs pollutant concentration ($[(\text{RH}_2)_{aq}]$) and (b) $1/\text{QY}$ vs $1/[(\text{RH}_2)_{aq}]$, under different illumination intensities, according to eq 18 ($k_{red}[\text{O}_2] = 10^{-3} \text{ cm s}^{-1}$, $k_o = 10^{-3}$, $k_{r1} = 10^{-8} \text{ cm}^3 \text{ s}^{-1}$, $k_{ox,1}^i = 10^{-18} \text{ cm}^3 \text{ s}^{-1}$).

oxidation of RH_2 dissolved species via surface-bound OH_s^* radicals (eq 5).

As discussed above, in the absence of specific adsorption the probability of direct hole transfer can be considered in general to be negligible, so that the quantum yield for RH_2 photooxidation can be defined as

$$\text{QY} = \frac{\text{molecules of R produced}}{\text{absorbed photons}} = \frac{\text{molecules of } \text{RH}_2 \text{ oxidized}}{\text{photogenerated holes}} = \frac{v_{ox,1}^i}{v_0} = \frac{k_{ox,1}^i[(\text{RH}_2)_{aq}][\text{OH}_s^*]}{k_0\phi} \quad (22)$$

At the quasi-steady-state we have that

$$\frac{d[\text{OH}_s^*]}{dt} = v_1 - v_{ox,1}^i - v_{ox,2}^i - v_{r1} = 0 \quad (23)$$

If we take into account that the RH_{aq}^* species does not accumulate, it must be $v_{ox,1}^i \approx v_{ox,2}^i$, and therefore:

$$[\text{OH}_s^*] \approx \{[(k_{ox,1}^i k_{red}[\text{O}_2][(\text{RH}_2)_{aq}])^2 + 2k_{ox,1}^i k_{r1} k_{red}[\text{O}_2][(\text{RH}_2)_{aq}] k_0\phi]^{1/2} - k_{ox,1}^i k_{red}[\text{O}_2][(\text{RH}_2)_{aq}]\} / \{2k_{ox,1}^i k_{r1}[(\text{RH}_2)_{aq}]\} \quad (24)$$

Finally, by substituting eq 24 into eq 22 the following expression for the quantum yield is obtained

$$QY = \left[\left(\frac{k_{ox,1}^i k_{red}[O_2][(RH_2)_{aq}]}{2k_{r_1} k_0 \phi} \right)^2 + \frac{k_{ox,1}^i k_{red}[O_2][(RH_2)_{aq}]}{2k_{r_1} k_0 \phi} \right]^{1/2} - \frac{k_{ox,1}^i k_{red}[O_2][(RH_2)_{aq}]}{2k_{r_1} k_0 \phi} \quad (25)$$

According to eq 25 $QY \rightarrow 1/2$ for $\phi \rightarrow 0$. Besides, for high enough illumination intensity, ($\phi \gg k_{ox,1}^i k_{red}[O_2][(RH_2)_{aq}]/2k_{r_1} k_0$), the quantum yield becomes:

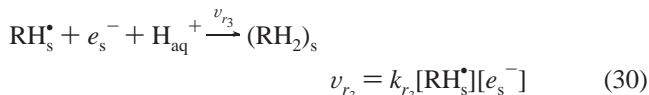
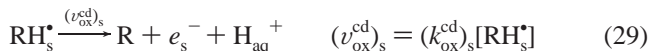
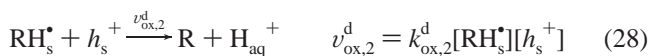
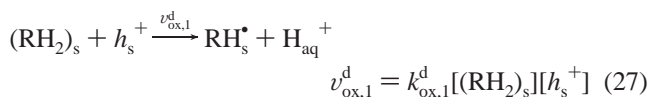
$$QY = \left[\frac{k_{ox,1}^i k_{red}[O_2][(RH_2)_{aq}]}{2k_0 k_{r_1}} \right]^{1/2} \phi^{-1/2} \quad (26)$$

Equations 25 and 26 are analogous to eqs 18 and 19, respectively, the differences being in constant factors. The dependence of the quantum yield on light intensity and on pollutant concentration is the same as in the presence of current doubling.

2C. Considering Other Competitive Reactions. If oxygen evolution is also considered to take place (eqs 2 to 4) an equation of third order in the surface concentration of photogenerated hydroxyl radicals ($[OH_s^*]$) is obtained under quasi-steady-state conditions. Of course, under particular circumstances this equation can be simplified. For instance, if we assume that most of electrons are used for reducing dissolved oxygen (i.e., $k_{r,1}[OH_s^*] \ll k_{red}[O_2]$) and that the light intensity is high enough, the third-order equation in $[OH_s^*]$ becomes a second-order equation, and the quantum yield becomes proportional to the square root of the light intensity, both in the presence and in the absence of the current doubling. Moreover, for $\phi \rightarrow 0$ the QY tends to 1 in the presence of current doubling and to 1/2 in its absence.

3. Specific Adsorption

The photooxidation of surface-bound $(RH_2)_s$ species is considered to take place via valence band free holes; the reaction scheme should now include:



Moreover, we have to consider the simultaneous photooxidation of nonadsorbed $(RH_2)_{aq}$ species via an indirect hole transfer mechanism involving eqs 1–8. As in the preceding cases, this is a simplified reaction scheme that does not include other secondary mechanisms of photooxidation for the dissolved pollutant species, such as those taking place in the bulk solution with the participation of oxidizing OH^* and H_2O_2 species generated at intermediate steps of the electroreduction of dissolved oxygen. Since $[(RH_2)_s]_{in} = [RH_s^*] + [(RH_2)_s]$, where $[(RH_2)_s]_{in}$ represents the initial concentration of surface-

bound $(RH_2)_s$ species under equilibrium conditions in the dark, it can be assumed that under low enough illumination intensity (standard experimental conditions) $[RH_2]_s \gg [RH_s^*]$ and $[(RH_2)_s]_{in} \approx [(RH_2)_s]$.

Equation 27 describes the rate of inelastic, direct photooxidation of surface-bound $(RH_2)_s$ species via valence band free holes, at a rate $\nu_{ox,1}^d$. Photogenerated surface-bound RH_s^* radicals are further photooxidized either via an inelastic direct mechanism, at a rate $\nu_{ox,2}^d$ given by eq 28, or via a “current doubling” mechanism, at a rate $(\nu_{ox}^{cd})_s$ defined by eq 29. Finally, eq 30 describes the inelastic recombination of free conduction band electrons with photogenerated surface-bound RH_s^* radicals (back reaction of 27), at a rate ν_{r_3} . Observe that reactions 29 and 30 are incompatible with each other because an efficient “current doubling” mechanism implicates a good overlapping of the filled energy levels associated with RH_s^* species with empty conduction band energy levels above E_c , so that the downhill recombination reaction (eq 30) becomes hindered. Although we have assumed that direct hole transfer generally applies to specifically adsorbed pollutant species, the previous reaction scheme is also valid for the case of nonspecific adsorption through replacement of $[(RH_2)_s]_{in}$ by $[(RH_2)_{aq}]$ and of $[RH_s^*]$ by $[RH_{aq}^*]$. In the latter case, reactions 27, 28, and 30 would be isoenergetic instead of inelastic.

Considering that direct photooxidation of surface-bound pollutant species coexists with indirect photooxidation of nonadsorbed species, the photodegradation quantum yield in this case should be written as

$$QY = \frac{R \text{ produced}}{\text{photons adsorbed}} = \frac{RH_2 \text{ consumed}}{\text{generated holes}} = \frac{\nu_{ox,2}^d + \nu_{ox,2}^d + (\nu_{ox}^{cd})_s + \nu_{ox}^{cd}}{k_0 \phi} = \frac{\nu_{ox,1}^d + \nu_{ox,1}^d - \nu_{r_3}}{k_0 \phi} = \frac{(k_{ox,1}^d [(RH_2)_s][h_s^+] + k_{ox,1}^d [(RH_2)_{aq}][OH_s^*] - k_{r_3} [RH_s^*][e_s^-])}{k_0 \phi} \quad (31)$$

Two main cases can be considered.

3A. Presence of Current Doubling: $\nu_{ox,2}^d = 0$, $\nu_{ox,2}^d = 0$ and $\nu_{r_3} = 0$. Equation 31 becomes

$$QY = \frac{\nu_{ox,1}^d + \nu_{ox,1}^d}{k_0 \phi} = \frac{k_{ox,1}^d [(RH_2)_s][h_s^+] + k_{ox,1}^d [(RH_2)_{aq}][OH_s^*]}{k_0 \phi} \quad (32)$$

with

$$[OH_s^*] \approx \{2k_0(C - E)\phi - D[(RH_2)_{aq}] + [(D[(RH_2)_{aq}] + 2k_0(E - C)\phi)^2 + 8B[(RH_2)_{aq}]Fk_0\phi]^{1/2}\} / \{4B[(RH_2)_{aq}]\}$$

where $A = k_1[OH_s^-] + k_{ox,1}^d [(RH_2)_s]$, $B = k_{ox,1}^i A k_{r_1}$, $C = k_1[OH_s^-] k_{r_1}$, $D = k_{ox,1}^i A k_{red}[O_2]$, $E = A k_{r_1}$, and $F = k_1[OH_s^-] k_{red}[O_2]$ (see Appendix A), so that eq 32 becomes:

$$QY \approx \frac{k_{ox,1}^d [(RH_2)_s]}{(k_1 [OH_s^-] + k_{ox,1}^d [(RH_2)_s])} + \frac{k_{ox,1}^i}{4Bk_0} \times \left[\left[\left(\frac{D[(RH_2)_{aq}] + 2k_0(E-C)\phi}{\phi} \right)^2 + \frac{8BFk_0[(RH_2)_{aq}]}{\phi} \right]^{1/2} - \frac{D[(RH_2)_{aq}] + 2k_0(E-C)\phi}{\phi} \right] \quad (33)$$

Let us now inspect the influence of the type of adsorption on the quantum yield. If a Langmuir adsorption isotherm is assumed, the relationship between the concentration of adsorbed and dissolved species will be

$$[(RH_2)_s]_{in} = \frac{ab[(RH_2)_{aq}]}{1 + a[(RH_2)_{aq}]} \quad (34)$$

a being the adsorption constant and b the surface concentration of adsorption sites, $[X_s]$. By combining eqs 33 and 34, the following quantum yield dependence on the concentration of dissolved pollutant species is obtained

$$QY \approx \left[\frac{k_{ox,1}^d [(RH_2)_{aq}] ab}{(k_1 a [OH_s^-]_{in} + ab k_{ox,1}^d [(RH_2)_{aq}] + k_1 [OH_s^-]_{in})} + \frac{\left[\frac{k_{ox,1}^i}{4Bk_0} \left[\left(\frac{D[(RH_2)_{aq}] + 2k_0(E-C)\phi}{\phi} \right)^2 + \frac{8BFk_0[(RH_2)_{aq}]}{\phi} \right]^{1/2} - \frac{D[(RH_2)_{aq}] + 2k_0(E-C)\phi}{\phi} \right]}{\phi} \right] \quad (35)$$

A similar reasoning would be valid for other adsorption isotherms.

The first term of eq 35 represents the light intensity independent contribution of direct hole transfer to the quantum yield, while the second term represents the illumination intensity dependent contribution of indirect hole transfer, which resembles eq 19 (i.e., QY is proportional to ϕ^{-m} , with $m \rightarrow 0$ for $\phi \rightarrow 0$). Of course, if RH_2 species adsorb at saturation blocking all the X_s sites, the direct mechanism would be the only one taking place irrespective of illumination intensity. If this is not the case, under low enough illumination intensity, indirect hole transfer will be predominant, since the second term increases toward unity as ϕ decreases while the first term is constant. By contrast, under high enough illumination intensity direct hole transfer will prevail for either strong enough adsorption of RH_2 species (high enough a , b constants in eq 34, so that $[(RH_2)_s]_{in} \gg [OH_s^-]_{in}$) and/or high enough $k_{ox,1}^d/k_{ox,1}^i$ rate constant ratio. Figure 5a shows a plot of the quantum yield vs illumination intensity according to eq 35. The corresponding contributions to the quantum yield of direct hole transfer (first term) and indirect hole transfer (second term) are shown in Figure 5, panels b and c, respectively. Figure 6 shows the influence of the pollutant concentration on the illumination intensity dependence of the quantum yield according to eq 35. It can be seen from Figures 5 and 6 that, in fact, for low enough illumination intensity ($\phi \leq 10^{11} \text{ cm}^{-2} \text{ s}^{-1}$), such that $v_{r1} \ll v_{ox,1}^i$, the second term (indirect hole transfer) prevails on the first one (direct hole transfer), and a light intensity quantum yield dependence similar to that predicted by eq 19 is observed (see Figures 2a and 3a). Moreover, under standard experimental conditions (high enough illumination intensity) the direct hole transfer term prevails over the indirect one and a light independent quantum yield is found. The actual quantum yield under constant illumination intensity

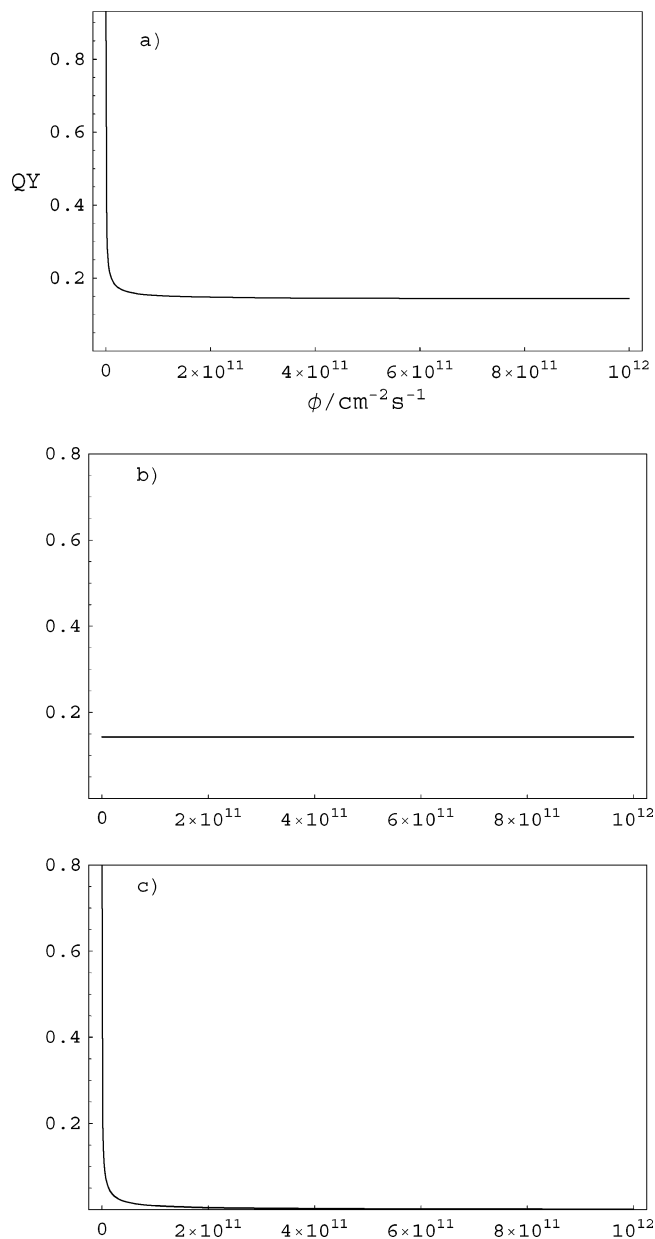


Figure 5. (a) Quantum yield (QY) vs illumination intensity (ϕ) plot, according to eq 35. The influence of the direct hole transfer and indirect hole transfer term are shown in (b) and (c), respectively ($a = 10^{-18} \text{ cm}^{-3}$, $b = 10^{14} \text{ cm}^{-2}$, $k_{ox,1}^d = k_1 = k_{r1} = 10^{-8} \text{ cm}^3 \text{ s}^{-1}$, $k_0 = 10^{-3}$, $[OH_s^-]_{in} = 5 \times 10^{14} \text{ cm}^{-2}$, $k_{red}[O_2] = 10^{-3} \text{ cm}^3 \text{ s}^{-1}$, $[(RH_2)_{aq}] = 10^{18} \text{ cm}^{-3}$ and $k_{ox,1}^i = 10^{-18} \text{ cm}^3 \text{ s}^{-1}$).

increases with $[(RH_2)_{aq}]$. The influence of the indirect hole transfer rate constant ($k_{ox,1}^i$) on the illumination intensity dependence of the quantum yield, according to eq 35, is shown in Figure 7. As for the case of eq 19, the lower $k_{ox,1}^i$ the lower the ϕ values where the direct hole transfer mechanism prevails over the indirect one and, therefore, a light intensity independent quantum yield is obtained. The influence of the indirect hole transfer rate constant ($k_{ox,1}^i$) on the inverse of the square root illumination intensity dependence of the quantum yield, according to eq 35, is shown in Figure 8. In agreement with the behavior shown in Figure 7, for low enough values of $k_{ox,1}^i$ indirect hole transfer prevails over direct hole transfer and $QY \propto \phi^{-1/2}$. Finally, the influence of the indirect hole transfer rate constant on the pollutant concentration dependence of the quantum yield, according to eq 35, is shown in Figure 9. As

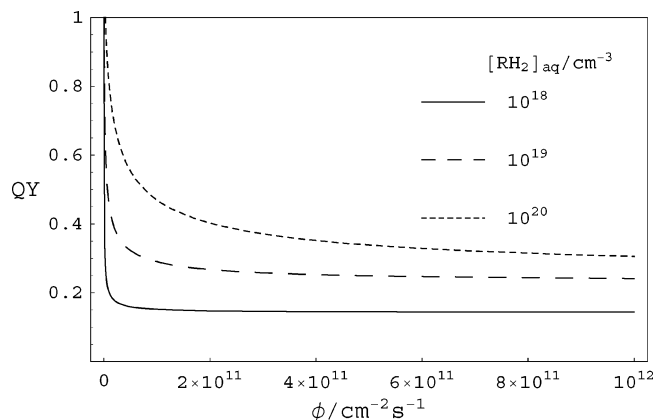


Figure 6. Influence of the pollutant concentration ($[(\text{RH}_2)_{\text{aq}}]$) on the illumination intensity (ϕ) dependence of the quantum yield (QY), according to eq 35, for $k_{\text{red}}[\text{O}_2] = 10^{-3} \text{ cm s}^{-1}$, $k_o = 10^{-3}$, $a = 10^{-18} \text{ cm}^{-3}$, $b = 10^{14} \text{ cm}^{-2}$, $k_{\text{ox},1}^{\text{d}} = k_1 = k_{\text{ox},1}^{\text{i}} = k_{\text{r}_1} = 10^{-8} \text{ cm}^3 \text{ s}^{-1}$, $[\text{OH}_s^-]_{\text{in}} = 3 \times 10^{14} \text{ cm}^{-2}$ and $k_{\text{ox},1}^{\text{i}} = 10^{-18} \text{ cm}^3 \text{ s}^{-1}$.

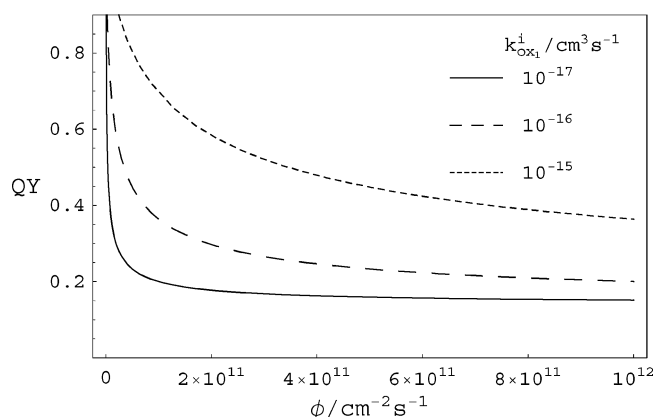


Figure 7. Influence of the indirect hole transfer rate constant ($k_{\text{ox},1}^{\text{i}}$) on the illumination intensity (ϕ) dependence of the quantum yield (QY), according to eq 35, for $k_{\text{red}}[\text{O}_2] = 10^{-3} \text{ cm s}^{-1}$, $k_o = 10^{-3}$, $a = 10^{-18} \text{ cm}^{-3}$, $b = 10^{14} \text{ cm}^{-2}$, $k_1 = k_{\text{ox},1}^{\text{d}} = k_{\text{r}_1} = k_{\text{r}_3} = 10^{-8} \text{ cm}^3 \text{ s}^{-1}$, $[\text{OH}_s^-]_{\text{in}} = 3 \times 10^{14} \text{ cm}^{-2}$ and $[(\text{RH}_2)_{\text{aq}}] = 10^{18} \text{ cm}^{-3}$.

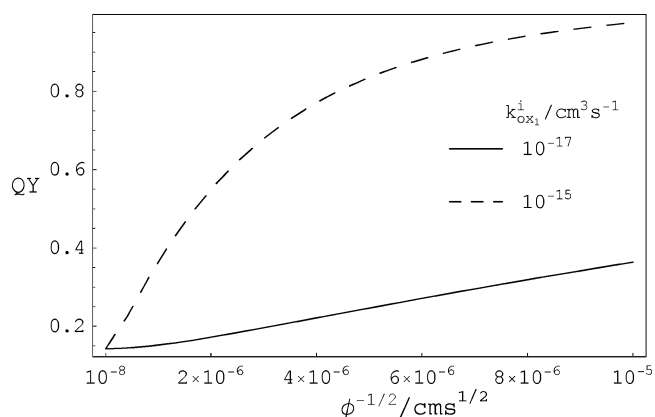


Figure 8. Predicted influence of the direct hole transfer rate constant, $k_{\text{ox},1}^{\text{d}}$, on the quantum yield (QY) dependence on the inverse of the illumination intensity square root ($\phi^{-1/2}$), according to eq 35, for: $a = 10^{-18} \text{ cm}^{-3}$, $b = 10^{14} \text{ cm}^{-2}$, $k_1 = k_{\text{ox},1}^{\text{d}} = k_{\text{r}_1} = k_{\text{r}_3} = 10^{-8} \text{ cm}^3 \text{ s}^{-1}$, $k_o = 10^{-3}$, $[\text{OH}_s^-]_{\text{in}} = 5 \times 10^{14} \text{ cm}^{-2}$, $k_{\text{red}}[\text{O}_2] = 10^{-3} \text{ cm s}^{-1}$ and $[(\text{RH}_2)_{\text{aq}}] = 10^{18} \text{ cm}^{-3}$.

expected, direct hole transfer (first term of eq 35) is prevalent, the quantum yield dependence on $[(\text{RH}_2)_{\text{aq}}]$ being that corresponding to the Langmuir behavior $((\text{QY})^{-1} \propto [(\text{RH}_2)_{\text{aq}}]^{-1})$ for low enough $[(\text{RH}_2)_{\text{aq}}]$ and/or low enough $k_{\text{ox},1}^{\text{i}}$.

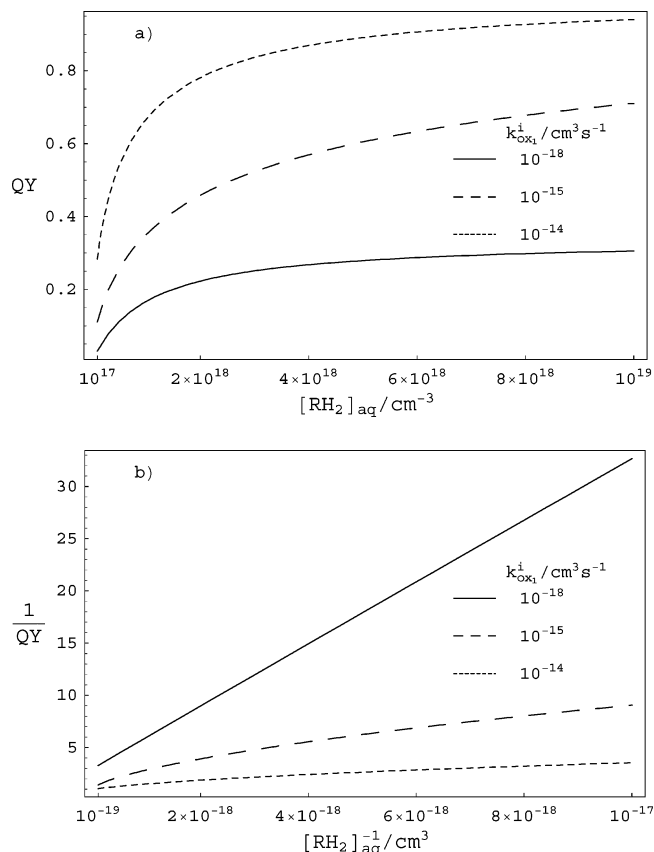


Figure 9. Influence of the indirect hole transfer rate constant ($k_{\text{ox},1}^{\text{i}}$) on (a) quantum yield (QY) dependence of the pollutant concentration ($[(\text{RH}_2)_{\text{aq}}]$), (b) $1/\text{QY}$ dependence on $1/[(\text{RH}_2)_{\text{aq}}]$ ($\phi = 10^{12} \text{ cm}^{-2} \text{ s}^{-1}$, $k_{\text{red}}[\text{O}_2] = 10^{-3} \text{ cm s}^{-1}$, $k_o = 10^{-3}$, $a = 10^{-18} \text{ cm}^{-3}$, $b = 10^{14} \text{ cm}^{-2}$, $k_1 = k_{\text{ox},1}^{\text{d}} = k_{\text{r}_1} = k_{\text{r}_3} = 10^{-8} \text{ cm}^3 \text{ s}^{-1}$ and $[\text{OH}_s^-]_{\text{in}} = 5 \times 10^{14} \text{ cm}^{-2}$).

3B. Absence of Current Doubling: $v_{\text{ox}}^{\text{cd}} = 0$ and $(v_{\text{ox}}^{\text{cd}})_s = 0$. In this case, eq 31 is still valid, so that under quasi-steady-state conditions the quantum yield can be rewritten as:

$$\text{QY} = \frac{v_{\text{ox},1}^{\text{d}} + v_{\text{ox},1}^{\text{i}} - v_{\text{r}_3}}{k_o \phi} = \frac{k_{\text{ox},1}^{\text{d}}[(\text{RH}_2)_s][h_s^+] + k_{\text{ox},1}^{\text{i}}[(\text{RH}_2)_{\text{aq}}][\text{OH}_s^*] - k_{\text{r}_3}[\text{RH}_s^*][e_s^-]}{k_o \phi} \quad (36)$$

Moreover,

$$\frac{d[h_s^+]}{dt} = v_0 - v_1 - v_{\text{ox},1}^{\text{d}} - v_{\text{ox},2}^{\text{d}} = 0 \quad (37)$$

so that

$$[h_s^+] \approx \frac{v_0}{k_1[\text{OH}_s^-]_{\text{in}} + k_{\text{ox},1}^{\text{d}}[(\text{RH}_2)_s]_{\text{in}} + k_{\text{ox},2}^{\text{d}}[\text{RH}_s^*]} \quad (38)$$

But under low enough illumination intensity (standard experimental conditions) it is $[(\text{RH}_2)_s]_{\text{in}} \approx [(\text{RH}_2)_s] \gg [\text{RH}_s^*]$, and $[\text{OH}_s^-] \approx [\text{OH}_s^-]_{\text{in}}$, and assuming comparable values for the rate constants $k_{\text{ox},1}^{\text{d}}$ and $k_{\text{ox},2}^{\text{d}}$, it will be $v_{\text{ox},1}^{\text{d}} \gg v_{\text{ox},2}^{\text{d}}$, and eq 38 becomes

$$[h_s^+] \approx \frac{\nu_0}{k_1[\text{OH}_s^-]_{\text{in}} + k_{\text{ox},1}^d[(\text{RH}_2)_s]_{\text{in}}} \quad (39)$$

Implicitly, we are assuming that most RH_s^* species will suffer recombination. However, if one assumes that they are further oxidized to R, the hole concentration would be somewhat smaller (its minimum value would be $[h_s^+] = \nu_0/(k_1[\text{OH}_s^-]_{\text{in}} + 2k_{\text{ox},1}^d[(\text{RH}_2)_s]_{\text{in}})$.

On the other hand,

$$\frac{d[e_s^-]}{dt} = \nu_0 - \nu_{r_1} - \nu_{r_3} - \nu_{\text{red}} = 0 \quad (40)$$

so that

$$[e_s^-] \approx \frac{\nu_0}{k_{r_1}[\text{OH}_s^*] + k_{r_3}[\text{RH}_s^*] + k_{\text{red}}[\text{O}_2]} \quad (41)$$

From a comparison of eqs 39 and 41, it is inferred that $[h_s^+] \ll [e_s^-]$, as for the case of non-specific adsorption (eqs 11 and 14)

Two different cases can now be considered: (i) surface recombination mainly takes place via photogenerated OH_s^* radicals (i.e., $\nu_{r_1} \gg \nu_{r_3}$); (ii) both OH_s^* and RH_s^* surface-bound photogenerated species participate in the recombination process. In case (i) eq 32 is valid, the quantum yield being defined by a light independent expression identical to eq 35. On the other hand, in case (ii), where ν_{r_3} cannot be neglected, eq 31 is valid. The combination of eqs 31, 39, and 41 leads to the following expression for the quantum yield:

$$\text{QY} \approx \frac{k_{\text{ox},1}^d[(\text{RH}_2)_s]_{\text{in}}}{k_1[\text{OH}_s^-]_{\text{in}} + k_{\text{ox},1}^d[(\text{RH}_2)_s]_{\text{in}}} + \frac{k_{\text{ox},1}^i[(\text{RH}_2)_{\text{aq}}]}{k_0\phi}[\text{OH}_s^*] - \frac{k_{r_3}[\text{RH}_s^*]}{k_{r_3}[\text{RH}_s^*] + k_{r_1}[\text{OH}_s^*] + k_{\text{red}}[\text{O}_2]} \quad (42)$$

By combining eqs 42 and 34 the quantum yield finally becomes

$$\text{QY} \approx \frac{k_{\text{ox},1}^d[(\text{RH}_2)_{\text{aq}}]ab}{(k_1a[\text{OH}_s^-]_{\text{in}} + abk_{\text{ox},1}^d)[(\text{RH}_2)_{\text{aq}}] + k_1[\text{OH}_s^-]_{\text{in}}} + \frac{k_{\text{ox},1}^i[(\text{RH}_2)_{\text{aq}}][\text{OH}_s^*]}{k_0\phi} - \frac{k_{r_3}[\text{RH}_s^*]}{k_{r_3}[\text{RH}_s^*] + k_{r_1}[\text{OH}_s^*] + k_{\text{red}}[\text{O}_2]} \quad (43)$$

Numerical solutions for $[\text{OH}_s^*](\phi)$ and $[\text{RH}_s^*](\phi)$ needed for solving eq 43 are given in Appendix B. The first term of eq 43, which represents the contribution of direct hole transfer to the quantum yield, is light intensity independent, while both the second term (indirect hole transfer contribution), which is similar to its homologous in eq 35, and the third term (contribution of recombination via RH_s^* species) decrease as ϕ increases. Figure 10a shows a plot of the quantum yield vs illumination intensity, according to eq 43. The contributions to the quantum yield of direct hole transfer (first term) and indirect hole transfer (second term) are shown in Figure 10, panels b and c, respectively, while the recombination term is shown in panel d. The behavior predicted by eq 42 is similar to that of eq 35, i.e., for low enough illumination intensity the second and third term of eq 43 prevail on the first one and the quantum yield decreases as ϕ increases. By contrast, under standard experimental conditions (high enough illumination intensity) direct hole transfer (first term) becomes dominant and a light independent quantum yield is found. Figure 11 shows the influence of the recombination rate

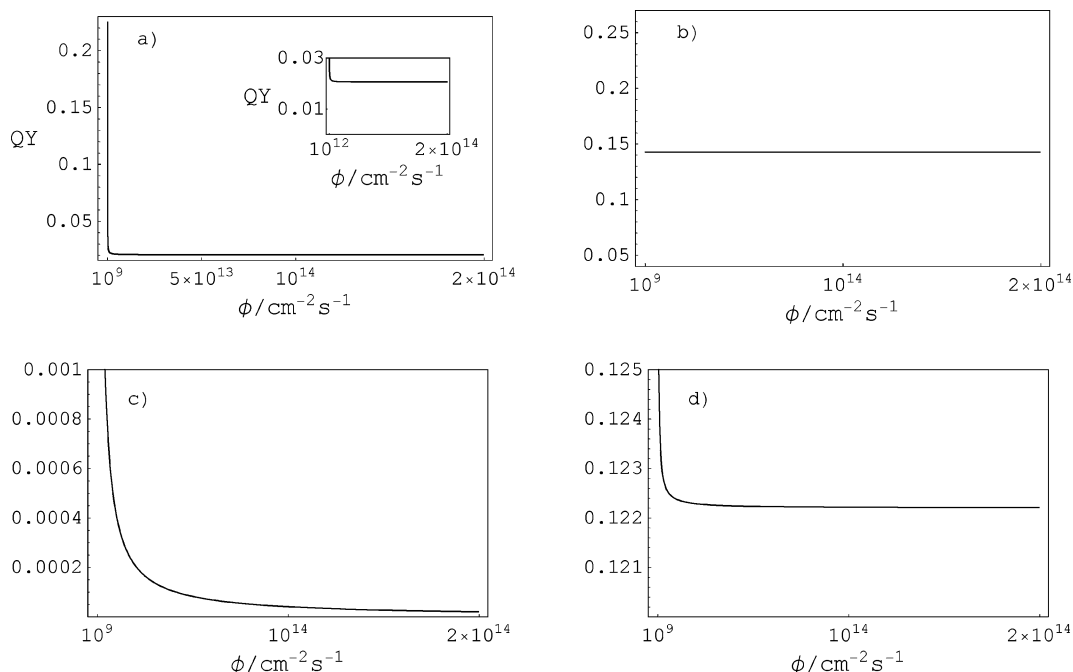


Figure 10. (a) Quantum yield (QY) vs illumination intensity (ϕ) plots, according to eq 43. The influence of the direct hole transfer, indirect hole transfer, and recombination term via RH_s^* intermediate species term are shown in (b), (c), and (d), respectively ($k_{\text{red}}[\text{O}_2] = 10^{-3} \text{ cm}^3 \text{ s}^{-1}$, $k_0 = 10^{-3}$, $a = 10^{-18} \text{ cm}^{-3}$, $b = 10^{14} \text{ cm}^{-2}$, $k_1 = k_{\text{ox},1}^d = k_{r_1} = k_{r_3} = 10^{-8} \text{ cm}^3 \text{ s}^{-1}$, $[\text{OH}_s^-]_{\text{in}} = 3 \times 10^{14} \text{ cm}^{-2}$, $[(\text{RH}_2)_{\text{aq}}] = 10^{18} \text{ cm}^{-3}$ and $k_{\text{ox},1}^i = 10^{-18} \text{ cm}^3 \text{ s}^{-1}$).

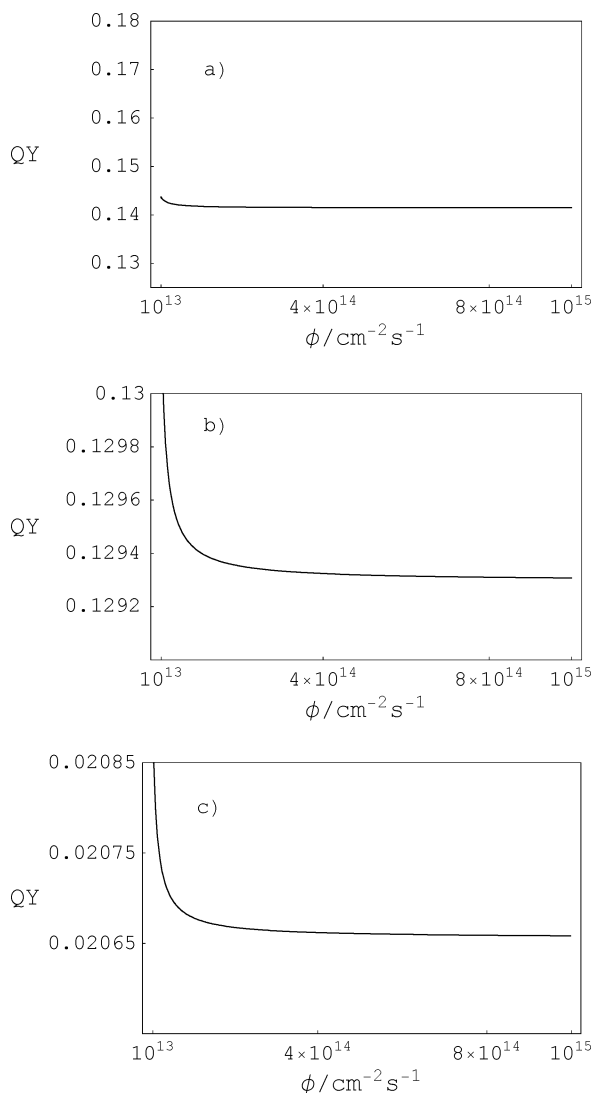


Figure 11. Influence of the recombination rate constant via RH_s^* photogenerated species (k_{r3}) on the illumination intensity (ϕ) dependence of the quantum yield (QY), according to eq 43, for $k_{r3} = 10^{-6} \text{ cm}^3 \text{s}^{-1}$ (a), $k_{r3} = 10^{-7} \text{ cm}^3 \text{s}^{-1}$ (b), $k_{r3} = 10^{-8} \text{ cm}^3 \text{s}^{-1}$ (c) and $k_{\text{red}}[\text{O}_2] = 10^{-3} \text{ cm}^3 \text{s}^{-1}$, $k_o = 10^{-3}$, $a = 10^{-18} \text{ cm}^{-3}$, $b = 10^{14} \text{ cm}^{-2}$, $k_1 = k_{\text{ox},1}^d = k_{r1} = 10^{-8} \text{ cm}^3 \text{s}^{-1}$, $k_{\text{ox},1}^i = 10^{-18} \text{ cm}^3 \text{s}^{-1}$, $[\text{OH}_s^-]_{\text{in}} = 3 \times 10^{14} \text{ cm}^{-2}$ and $[(\text{RH}_2)_{\text{aq}}] = 10^{18} \text{ cm}^{-3}$.

constant via RH_s^* photogenerated species (k_{r3}) on the illumination intensity dependence of the quantum yield, according to eq 43. As can be seen, the higher k_{r3} the lower the ϕ values where direct hole transfer (first term) is prevalent. The influence of the indirect hole transfer rate constant ($k_{\text{ox},1}^i$) on the illumination intensity dependence of the quantum yield, according to eq 43, is shown in Figure 12. As expected, the predicted behavior is similar to that of eq 35 (Figure 7), i.e., the lower the value of $k_{\text{ox},1}^i$ the lower the ϕ values where direct hole transfer is prevalent and a light intensity independent quantum yield is obtained. Figure 13a shows the influence of the illumination intensity on the pollutant concentration dependence of the quantum yield, while Figure 13b shows the influence of the illumination intensity on the inverse pollutant concentration dependence of the reciprocal of the quantum yield, according to eq 43. As expected, the Langmuir behavior ($\text{QY}^{-1} \propto [(\text{RH}_2)_{\text{aq}}]^{-1}$) characteristic of direct hole transfer is observed for low enough $[(\text{RH}_2)_{\text{aq}}]$ and/or high enough ϕ values ($[(\text{RH}_2)_{\text{aq}}]^{-1} \leq 2 \times 10^{-18} \text{ cm}^3$ for $\phi = 10^{15} \text{ cm}^{-2} \text{s}^{-1}$ and

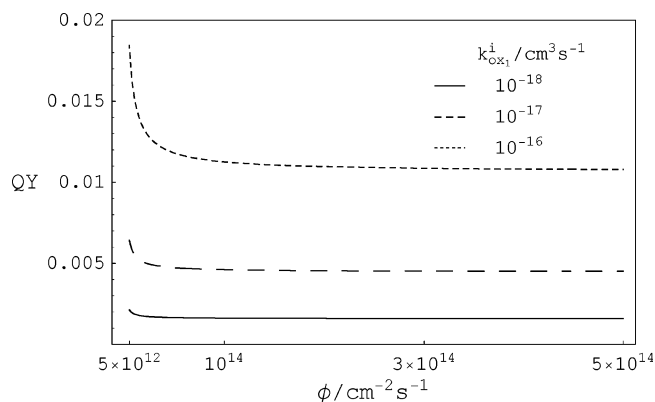


Figure 12. Influence of the indirect hole transfer rate constant ($k_{\text{ox},1}^i$) on the illumination intensity (ϕ) dependence of the quantum yield (QY), according to eq 43, for $a = 10^{-18} \text{ cm}^{-3}$, $b = 10^{14} \text{ cm}^{-2}$, $k_1 = k_{\text{ox},1}^d = k_{r1} = k_{r3} = 10^{-8} \text{ cm}^3 \text{s}^{-1}$, $k_o = 10^{-3}$, $[\text{OH}_s^-]_{\text{in}} = 5 \times 10^{14} \text{ cm}^{-2}$, $k_{\text{red}}[\text{O}_2] = 10^{-3} \text{ cm}^3 \text{s}^{-1}$ and $[(\text{RH}_2)_{\text{aq}}] = 10^{17} \text{ cm}^{-3}$.

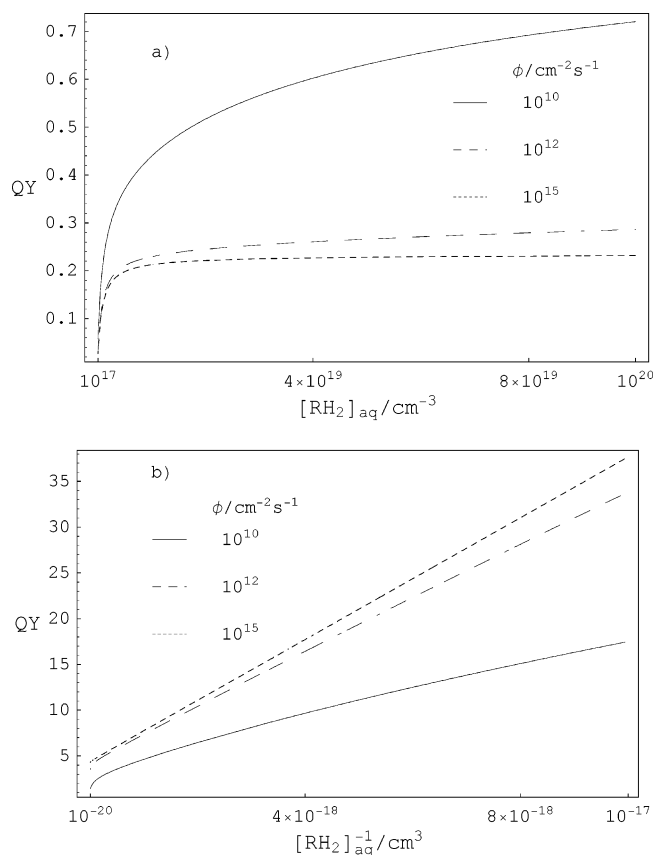


Figure 13. Predicted influence of the illumination intensity (ϕ), according to eq 43, on the dependence of (a) quantum yield on the pollutant concentration, (b) $1/\text{QY}$ on $1/[(\text{RH}_2)_{\text{aq}}]$ ($k_{\text{ox},1}^i = 10^{-18} \text{ cm}^3 \text{s}^{-1}$, $k_{\text{red}}[\text{O}_2] = 10^{-3} \text{ cm}^3 \text{s}^{-1}$, $k_o = 10^{-3}$, $a = 10^{-18} \text{ cm}^{-3}$, $b = 10^{14} \text{ cm}^{-2}$, $k_1 = k_{\text{ox},1}^d = k_{r1} = 10^{-8} \text{ cm}^3 \text{s}^{-1}$, $[\text{OH}_s^-]_{\text{in}} = 3 \times 10^{14} \text{ cm}^{-2}$, $k_{r3} = 10^{-7} \text{ cm}^3 \text{s}^{-1}$ and $\phi = 10^{10} \text{ cm}^{-2} \text{s}^{-1}$).

$[(\text{RH}_2)_{\text{aq}}]^{-1} \leq 6 \times 10^{-18} \text{ cm}^3$ for $\phi = 10^{10} \text{ cm}^{-2} \text{s}^{-1}$). Finally, the influence of the indirect hole transfer rate constant ($k_{\text{ox},1}^i$) on the pollutant concentration dependence of the quantum yield, according to eq 43 is shown in Figure 14a, while the influence of the indirect hole transfer rate constant ($k_{\text{ox},1}^i$) on the inverse pollutant concentration dependence of the reciprocal of the quantum yield is shown in Figure 14b. The behavior observed is identical to that predicted by eq 35 (Figure 9), i.e., the lower $[(\text{RH}_2)_{\text{aq}}]$ and/or the lower $k_{\text{ox},1}^i$ the more predominant is the

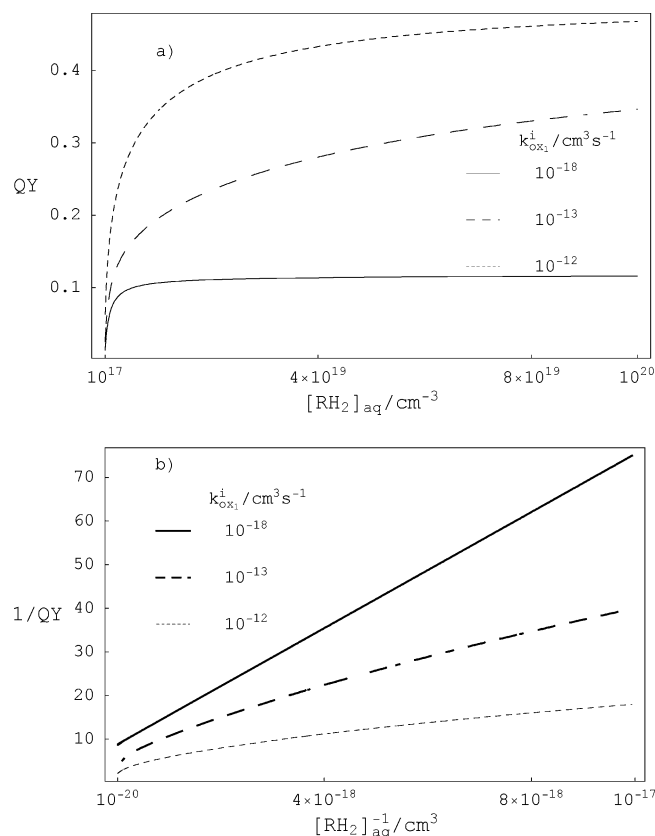


Figure 14. Predicted influence of the indirect hole transfer rate constant ($k_{ox,1}^i$), according to eq 43, on the dependence of (a) quantum yield (QY) on the pollutant concentration ($[(RH_2)_{aq}]$), (b) $1/QY$ on $1/[(RH_2)_{aq}]$ ($\phi = 10^{15} \text{ cm}^{-2} \text{ s}^{-1}$, $k_{red}[O_2] = 10^{-3} \text{ cm}^3 \text{ s}^{-1}$, $k_o = 10^{-3}$, $a = 10^{-18} \text{ cm}^{-3}$, $b = 10^{14} \text{ cm}^{-2}$, $k_1 = k_{ox,1}^d = k_{r1} = 10^{-8} \text{ cm}^3 \text{ s}^{-1}$, $k_{r3} = 10^{-7} \text{ cm}^3 \text{ s}^{-1}$, $[OH_s^-]_{in} = 5 \times 10^{14} \text{ cm}^{-2}$ and $\phi = 10^{15} \text{ cm}^{-2} \text{ s}^{-1}$).

direct hole transfer mechanism, so that a Langmuir behavior ($QY^{-1} \propto [(RH_2)_{aq}]^{-1}$) becomes more apparent.

4. Conclusions

The kinetic model here proposed for explaining the photocatalytic degradation of dissolved pollutant species at dispersions of TiO_2 nanoparticles is an implementation of a previous model developed for interpreting photoelectrochemical experiments.⁴⁹ This model emphasizes the important role that the interaction of the dissolved pollutant species with the semiconductor surface

plays in determining whether interfacial hole transfer takes place directly or indirectly. It establishes that an isoenergetic, indirect hole transfer mechanism prevails in the case of nonspecific adsorption of dissolved pollutant species, while direct hole transfer takes place inelastically under specific adsorption. In general, the direct mechanism involves a higher hole transfer rate than the indirect one. The main predictions of the model are summarized in Table 1. For indirect hole transfer, the model predicts a $QY \propto \phi^{-m}$ relation, with $0 \leq m \leq 1/2$, a $QY \propto \phi^{-1/2}$ dependence being obtained for high enough illumination intensity, while for low enough illumination intensity ($\phi \rightarrow 0$) $QY \rightarrow 1$ in the presence of current doubling. In the case of specific adsorption, direct and indirect hole transfer will coexist if both surface-bound pollutant species and water molecules compete for hole capture, and a mixed behavior will be obtained (i.e., $QY \propto \phi^{-m}$ for low enough illumination intensity and $QY = \text{const}$ for high enough light intensity). It can be concluded that under low enough illumination intensity (far below typical experimental conditions) the quantum yield will reach in general higher values under nonspecific adsorption than under specific adsorption. By contrast, under high enough illumination intensity (standard experimental conditions) the direct hole transfer mechanism will lead to higher quantum yield values, especially when some of the following conditions are fulfilled: (i) pollutant species are adsorbed more strongly than water molecules ($[(RH_2)_{s,in}] \gg [OH_s^-]_{in}$), (ii) the rate constant for transfer of photogenerated valence band free holes to $(RH_2)_s$ species is much higher than that to adsorbed water molecules ($k_{ox,1}^d \gg k_1$), (iii) the recombination rate constant via photogenerated surface-bound OH_s^\bullet radicals is much higher than that involving RH_s^\bullet radicals. Moreover, in the case of specific adsorption (direct hole transfer), the adsorption isotherm for the pollutant will have a remarkable influence on the pollutant concentration dependence of the quantum yield. So, for a Langmuir adsorption type, a linear dependence of the inverse of the QY on the inverse of the pollutant concentration ($QY^{-1} \propto [(RH_2)_{aq}]^{-1}$) is predicted, while $QY^{-1} \propto [(RH_2)_{aq}]^{-1/2}$ would occur for nonspecific adsorption (indirect hole transfer). These predictions have been contrasted with experimental results from the literature. For instance, in the photocatalytic oxidation of methanol,^{58,59} chloroform,⁶² methyl viologen⁶³ and substituted 1,3-dihydroxy benzenes,⁶⁴ 2-propanol,⁶⁵ indirect hole transfer seems to predominate, as $QY \propto \phi^{-1/2}$, while in the photooxidation of formic acid,⁴⁶ chlorophenol⁴⁷ and dimetil-pyrodine *N*-oxide,⁴⁸ acetic acid,⁶⁶ direct hole transfer seems to be the prevailing hole

TABLE 1: Summary of the Behavior of the Quantum Yield (QY) for the Photooxidation of Pollutant RH_2 Species as a Function of the Illumination Intensity (ϕ) and Pollutant Concentration ($[(RH_2)_{aq}]$) for Both Indirect Hole Transfer (IHT) and Direct Hole Transfer (DHT) Mechanisms

electronic interaction	transfer mechanism	QY dependence on ϕ	QY dependence on $[(RH_2)_{aq}]$	QY^{-1} dependence on $[(RH_2)_{aq}]^{-1}$
weak (nonspecific adsorption)	IHT	$QY \propto \phi^{-m}$ $m \rightarrow 1/2$ for high enough ϕ $m \rightarrow 0$ for $\phi \rightarrow 0$ (eq 18)	$QY \propto [(RH_2)_{aq}]^{1/2}$ (eq 18)	nonlinear (eq 18)
strong ^a (specific adsorption)	DHT	$QY = \text{const}$ (eqs 33 and 43)	$QY \propto A[(RH_2)_{aq}]/B[(RH_2)_{aq}] + C$ (for high enough ϕ and/or low enough $[(RH_2)_{aq}]$) (eqs 33 and 43)	linear (for high enough ϕ and/or low enough $[(RH_2)_{aq}]$) (eqs 33 and 43) nonlinear (for low enough ϕ and/or high enough $[(RH_2)_{aq}]$) (eqs 33 and 43)

^a IHT and DHT mechanisms can coexist in the case of specific adsorption; a mixed behavior is then obtained (see eqs 28 and 33 and Figures 4 and 7).

transfer mechanism as a light intensity independent quantum yield is apparently obtained.

Acknowledgment. Financial support from the European Union under contract ICA3-CT-1999-00016 and from DGI (MCYT, Spain) through project BQU2003-03737 is acknowledged. T.L. is grateful to the MECD (Spain) for the award of a FPU grant.

Appendix A

Under specific adsorption and “current doubling” the photodegradation quantum yield is defined as:

$$QY = \frac{v_{ox,1}^d + v_{ox,1}^i}{k_0\phi} = \frac{k_{ox,1}^d[(RH_2)_s][h_s^+] + k_{ox,1}^i[(RH_2)_{aq}][OH_s^*]}{k_0\phi} \quad (A.0)$$

but under quasi-steady-state conditions

$$\frac{d[h_s^+]}{dt} = v_0 - v_1 - v_3 - v_4 - v_{ox,1}^d \approx v_0 - v_1 - v_{ox,1}^d = 0$$

so that

$$[h_s^+] \approx \frac{v_0}{k_1[OH_s^-] + k_{ox,1}^d[(RH_2)_s]} \quad (A.1)$$

Moreover,

$$d[e_s^-]/dt = v_0 - v_{red} - v_{r_1} + v_{ox}^{cd} + (v_{ox}^{cd})_s = 0$$

so that

$$[e_s^-] = \{ (k_0\phi + k_{ox,1}^i[(RH_2)_{aq}][OH_s^*])(k_1[OH_s^-] + k_{ox,1}^d[(RH_2)_s]) + k_{ox,1}^d[(RH_2)_s]k_0\phi / \{ (k_{red}[O_2] + k_{r,1}[OH_s^*])(k_1[OH_s^-] + k_{ox,1}^d[(RH_2)_s]) \} \} \quad (A.2)$$

On the other hand,

$$\frac{d[OH_s^*]}{dt} = v_1 - v_{ox,1}^i - v_{r_1} = k_1[h_s^+][OH_s^-] - (k_{ox,1}^i[(RH_2)_{aq}] + k_{r_1}[e_s^-])[OH_s^*] = 0 \quad (A.3)$$

By combining eqs A.1, A.2, and A.3 we obtain:

$$2B[(RH_2)_{aq}][OH_s^*]^2 - (2k_0(C - E)\phi + D[(RH_2)_{aq}])[OH_s^*] - Fk_0\phi \approx 0$$

so that

$$[OH_s^*] \approx \{ 2k_0(C - E)\phi - D[(RH_2)_{aq}] + [(D[(RH_2)_{aq}] + 2k_0(E - C)\phi)^2 + 8B[(RH_2)_{aq}]Fk_0\phi]^{1/2} / \{ 4B[(RH_2)_{aq}] \} \} \quad (A.4)$$

with $A = k_1[OH_s^-] + k_{ox,1}^d[(RH_2)_s]$, $B = k_{ox,1}^iAk_{r,1}$, $C = k_1[OH_s^-]k_{r,1}$, $D = k_{ox,1}^iAk_{red}[O_2]$, $E = Ak_{r,1}$, and $F = k_1[OH_s^-]k_{red}[O_2]$. Therefore, by considering eqs A1 and A4, eq A0 becomes

$$QY \approx \frac{k_{ox,1}^d[(RH_2)_s]}{(k_1[OH_s^-] + k_{ox,1}^d[(RH_2)_s])} + \frac{k_{ox,1}^i}{4Bk_0} \times \left[\left[\left(\frac{D[(RH_2)_{aq}] + 2k_0(E - C)\phi}{\phi} \right)^2 + \frac{8BFk_0[(RH_2)_{aq}]}{\phi} \right]^{1/2} - \frac{D[(RH_2)_{aq}] + 2k_0(E - C)\phi}{\phi} \right] \quad (A.5)$$

Appendix B

Let us determine $[OH_s^*](\phi)$ and $[RH_s^*](\phi)$ in eq 43 under steady-state conditions. On one hand we have that

$$\frac{d[OH_s^*]}{dt} = v_1 - v_{ox,1}^i - v_{r_1} - v_{ox,2}^i = 0 \quad (B.0)$$

But under low enough illumination intensity (standard experimental conditions) it can be assumed that $v_1 \approx v_0 - v_{ox,1}^d$, eq B.0 becoming:

$$v_0 - k_{ox,1}^d[(RH_2)_s]_{in}[h_s^+] - (k_{ox,1}^i[(RH_2)_{aq}] + k_{r_1}[e_s^-])[OH_s^*] \approx 0 \quad (B.1)$$

On the other hand,

$$\frac{d[RH_s^*]}{dt} = v_{ox,1}^d - v_{ox,2}^d - v_{r_3} = k_{ox,1}^d[(RH_2)_s]_{in}[h_s^+] - k_{ox,2}^d[RH_s^*][h_s^+] - k_{r_3}[RH_s^*][e_s^-] = 0 \quad (B.2)$$

For obtaining $[h_s^+]$ from eq 39, it was considered $v_{ox,1}^d \gg v_{ox,2}^d$; otherwise, the difficulties for calculating the QY according to eq 43 increase dramatically. Although this approach is not valid for solving eq B.2, as it leads to the unrealistic conclusion that $v_{r_3} = v_{ox,1}^d$, which implicates total recombination via photogenerated RH_s^* species (i.e., $QY = 0$), we can adopt the reasonable compromise of combining eqs B.2 and 39, as it does not affect the predicted behavior of the system concerning the QY dependence on the experimental variables ϕ and $[(RH_2)_{aq}]$. In this case, the following nonlinear relationship between $[OH_s^*]$ and $[RH_s^*]$ is obtained

$$A[OH_s^*]^2 + (B\phi + C)[OH_s^*] + E[RH_s^*][OH_s^*] - D\phi[RH_s^*] - F\phi = 0 \quad (B.3)$$

with

$$A = k_{r_1}(k_1[OH_s^-]_{in} + k_{ox,1}^d[(RH_2)_s]_{in})k_{ox,1}^i[(RH_2)_{aq}], \\ B = k_{r_1}k_{ox,1}^d[(RH_2)_s]_{in}k_0, C = k_{red}[O_2](k_1[OH_s^-]_{in} + k_{ox,1}^d[(RH_2)_s]_{in})k_{ox,1}^i[(RH_2)_{aq}], \\ D = k_{r_3}k_1[OH_s^-]_{in}k_0, \\ E = k_{r_3}(k_1[OH_s^-]_{in} + k_{ox,1}^d[(RH_2)_s]_{in})k_{ox,1}^i[(RH_2)_{aq}], \text{ and} \\ F = k_{red}[O_2]k_1k_0[OH_s^-]_{in}$$

Moreover, by combining eq B.1 with eqs 39 and 41 we obtain:

$$G[RH_s^*]^2 + Hk_0[RH_s^*] + I[RH_s^*][OH_s^*] - K[OH_s^*] - L = 0 \quad (B.4)$$

with $G = k_{r3}k_{ox,2}^d k_0$, $H = (k_{red}[O_2]k_{ox,2}^d + k_{r3}k_1[OH_s^-]_{in})k_0$, $I = k_{r3}k_{ox,2}^d k_0$, $K = k_{r3}k_{ox,1}^d[(RH_2)_s]_{in}k_0$, and $L = k_{red}[O_2]k_{ox,2}^d - [(RH_2)_s]_{in}$

The numerical solution of the system of nonlinear equations in $[OH_s^-](\phi)$ and $[RH_2^*](\phi)$, B.3 and B.4, allows one to determine the quantum yield by using eq 43.

References and Notes

- (1) Blake, M. D. In *Heterogeneous Photocatalytic Removal of Hazardous Compounds from Water and Air*; NREL/TP-570-26797, National Renewable Energy Laboratory: Golden, Co., 1999; Update No. 4 to October 2001, NREL/TP-510-31319.
- (2) Gerischer, H. *Electrochim. Acta* **1993**, *38*, 3.
- (3) Turchi, C. S.; Ollis, D. F. *J. Catal.* **1990**, *122*, 178.
- (4) Minero, C.; Aliberti, C.; Pelizzetti, E.; Terzian, R.; Serpone, N. *Langmuir* **1991**, *7*, 928.
- (5) Hoffmann, M. R.; Martin, S. T.; Choi, W.; Bahnemann, D. W. *Chem. Rev.* **1995**, *95*, 69.
- (6) Schwarz, P. F.; Turro, N. J.; Bossmann, S. H.; Braun, A. M.; Wahab, A. A.; Dürr, H. *J. Phys. Chem. B* **1997**, *101*, 7127.
- (7) Fujishima, A.; Tryk, D. A. In *Encyclopedia of Electrochemistry, Vol. 6, Semiconductor Electrodes and Photoelectrochemistry*; Bard, A. J., Stratmann, M., Eds.; Wiley-VCH: Weinheim, 2001.
- (8) Gao, R.; Stark, J.; Bahnemann, D. W.; Rabani, J. *J. Photochem. Photobiol. A* **2002**, *148*, 387.
- (9) Draper, R. B.; Fox, M. A. *Langmuir* **1990**, *6*, 1396.
- (10) Chen, J.; Ollis, D. F.; Rulkens, W. H.; Bruning, H. *Water Res.* **1999**, *33*, 669.
- (11) Fan, J.; Yates, J. T. *J. Am. Chem. Soc.* **1996**, *118*, 4686.
- (12) Ishibashi, K.-I.; Fujishima, A.; Watanabe, T.; Hashimoto, K. *J. Photochem. Photobiol. A* **2000**, *134*, 139.
- (13) Mao, Y.; Schoeneich, C.; Asmus, K. D. *J. Phys. Chem.* **1991**, *95*, 10080.
- (14) Carraway, E. R.; Hoffman, A. J.; Hoffmann, M. R. *Environ. Sci. Technol.* **1994**, *28*, 786.
- (15) Bahnemann, D. W.; Hilgendorff, M.; Memming, R. *J. Phys. Chem. B* **1997**, *101*, 4265.
- (16) Milis, A.; Peral, J.; Domenech, X. *Oxid. Commun.* **1994**, *17*, 163.
- (17) Roméas, V.; Pichat, P.; Guillard, C.; Chopin, T.; Lehaut, C. *New J. Chem.* **1999**, *23*, 365.
- (18) Minero, C.; Mariella, G.; Maurino, V.; Pelizzetti, E. *Langmuir* **2000**, *16*, 2632.
- (19) Minero, C. *Catal. Today* **1999**, *54*, 205.
- (20) Goldstein, S.; Czapski, G.; Rabani, J. *J. Phys. Chem.* **1994**, *98*, 6586.
- (21) Kesselman, J. M.; Weres, O.; Lewis, N. S.; Hoffmann, M. R. *J. Phys. Chem. B* **1997**, *101*, 2637.
- (22) Khodja, A. A.; Sehili, T.; Pilichowski, J. F.; Boule, P. *J. Photochem. Photobiol. A* **2001**, *141*, 231.
- (23) Chiang, K.; Amal, R.; Tran, T. *J. Mol. Catal. A* **2003**, *193*, 285.
- (24) Cunningham, J.; Al-Sayed, G.; Srijaranai, S. In *Aquatic and Surface Photochemistry*; Gels, G., Zeep, R. G., Crosby, D. G., Eds.; Lewis, Boca Raton: FL, 1994; pp 317–348.
- (25) Gomes da Silva, C.; Faria, J. L. *J. Photochem. Photobiol. A* **2003**, *155*, 133.
- (26) Epling, G. A.; Lin, C. *Chemosphere* **2002**, *46*, 561.
- (27) Butler, E. C.; Davis, A. P. *J. Photochem. Photobiol. A* **1993**, *70*, 273.
- (28) Davis, A. P.; Huang, C. P. *Chemosphere* **1993**, *26*, 1119.
- (29) Jenny, B.; Pichat, P. *Langmuir* **1991**, *7*, 947.
- (30) Krosley, K. W.; Collard, D. M.; Adamson, J.; Fox, M. A. *J. Photochem. Photobiol. A* **1993**, *69*, 357.
- (31) Galindo, C.; Jacques, P.; Kalt, A. *J. Photochem. Photobiol. A* **2000**, *130*, 35.
- (32) Houas, A.; Lachheb, H.; Ksibi, M.; Elaloui, E.; Guillard, C.; Hermann, J.-M. *Appl. Catal. B* **2001**, *31*, 145.
- (33) Saquib, M.; Muneer, M. *Dyes Pigm.* **2003**, *56*, 37.
- (34) Xu, Y.; Langford, C. H. *Langmuir* **2001**, *17*, 897.
- (35) Milis, A.; Peral, J.; Domenech, X.; Navio, J. A. *J. Mol. Catal.* **1994**, *87*, 67.
- (36) Mills, A.; Morris, S. *J. Photochem. Photobiol. A* **1993**, *71*, 75.
- (37) Konstantinou, I. K.; Albanis, T. A. *Appl. Catal. B* **2004**, *49*, 1.
- (38) Trillas, M.; Peral, J.; Domenech, X. *Appl. Catal. B* **1993**, *3*, 45.
- (39) Emeline, A. V.; Ryabchuk, V.; Serpone, N. *J. Photochem. Photobiol. A* **2000**, *133*, 89.
- (40) Sauer, T.; Neto, G. C.; José, H. J.; Moreira, R. F. P. M. *J. Photochem. Photobiol. A* **2002**, *149*, 147.
- (41) Martin, S. T.; Herrmann, H.; Choi, W.; Hoffmann, M. R. *J. Chem. Soc., Faraday Trans.* **1994**, *90*, 3315.
- (42) Martin, S. T.; Herrmann, H.; Hoffmann, M. R. *J. Chem. Soc., Faraday Trans.* **1994**, *90*, 3323.
- (43) Alberty, W. J.; Brown, G. T.; Darwent, J. R.; Saievar-Iranizad, E. *J. Chem. Soc., Faraday Trans. I* **1985**, *81*, 1999.
- (44) Kormann, C.; Bahnemann, D. W.; Hoffmann, M. R. *Environ. Sci. Technol.* **1991**, *25*, 494.
- (45) Turchi, C. S.; Ollis, D. F. *J. Catal.* **1990**, *122*, 178.
- (46) Dijkstra, M. F. J.; Panneman, H. J.; Winkelman, J. G. M.; Kelly, J. J.; Beenackers, A. A. C. M. *Chem. Eng. Sci.* **2002**, *57*, 4895.
- (47) Ahmed, S.; Kemp, T. J.; Unwin, P. R. *J. Photochem. Photobiol. A* **2001**, *141*, 69.
- (48) Grela, M. A.; Coronel, M. E. J.; Colussi, A. J. *J. Phys. Chem.* **1996**, *100*, 16940.
- (49) Lana Villarrreal, T.; Gómez, R.; Neumann-Spallart, M.; Alonso-Vante, N.; Salvador, P. *J. Phys. Chem. B* **2004**, *108*, 15172.
- (50) Gerischer, H. *J. Phys. Chem.* **1991**, *95*, 1356.
- (51) Pelizzetti, E.; Minero, C. *Electrochim. Acta* **1993**, *38*, 47.
- (52) Grela, M. A.; Brusa, M. A.; Colussi, A. J. *J. Phys. Chem. B* **1999**, *103*, 6400.
- (53) Salvador, P.; García-González, M. L.; Muñoz, F. *J. Phys. Chem.* **1992**, *96*, 10349.
- (54) Gerischer, H.; Heller, A. *J. Phys. Chem.* **1991**, *95*, 5261.
- (55) Salvador, P. *New J. Chem.* **1988**, *12*, 35.
- (56) Gerischer, H. *Electrochim. Acta* **1995**, *40*, 1277.
- (57) Salvador, P. *J. Phys. Chem.* **1985**, *89*, 3863.
- (58) Wang, C.; Rabani, J.; Bahnemann, D. W.; Dohrmann, J. K. *J. Photochem. Photobiol. A* **2002**, *148*, 169.
- (59) Wang, C.; Bahnemann, D. W.; Dohrmann, J. K. *Wat. Sci. Technol.* **2001**, *44*, 279.
- (60) Ahmed, S.; Fonseca, S. M.; Kemp, T. J.; Unwin, P. R. *J. Phys. Chem. B* **2003**, *107*, 5892.
- (61) Kesselmann, J. M.; Shreve, G. A.; Hoffmann, M. R.; Lewis, N. S. *J. Phys. Chem.* **1994**, *98*, 13385.
- (62) Kormann, C.; Bahnemann, D. W.; Hoffmann, M. R. *Environ. Sci. Technol.* **1991**, *25*, 494.
- (63) Martyanov, I. N.; Savinov, E. N. *J. Photochem. Photobiol. A* **2000**, *134*, 219.
- (64) Ökte, A. N.; Resat, M. S.; Inel, Y. *J. Photochem. Photobiol. A* **2000**, *134*, 59.
- (65) Egerton, T. A.; King, C. J. *J. Oil Colour Chem. Assoc.* **1979**, *62*, 386.
- (66) Bideau, M.; Claudel, B.; Faure, L.; Kazouan, H. *J. Photochem. Photobiol. A: Chem.* **1991**, *61*, 269.